Colloquium: Hidden order, superconductivity, and magnetism: The unsolved case of URu_2Si_2

J. A. Mydosh*

Kamerlingh Onnes Laboratory, Leiden University, P.O. Box 9504, NL-2300 RA Leiden, The Netherlands

P. M. Oppeneer†

Department of Physics and Astronomy, Uppsala University, P.O. Box 516, S-75120 Uppsala, Sweden

(published 16 November 2011)

This Colloquium reviews the 25 year quest to understand the continuous (second-order), mean-field-like phase transition occurring at 17.5 K in URu_2Si_2. About ten years ago, the term "hidden order" (HO) was coined and has since been utilized to describe the unknown ordered state, whose origin cannot be disclosed by conventional solid-state probes, such as x rays, neutrons, or muons. The HO is able to support superconductivity at lower temperatures ($T_c \approx 1.5$ K), and when magnetism is developed with increasing pressure both the HO and the superconductivity are destroyed. Other ways of probing the HO are via Rh doping and large magnetic fields. During the last few years a variety of advanced techniques have been tested to probe the HO state and these attempts will be summarized. A digest of recent theoretical developments is also included. It is the objective of this Colloquium to shed additional light on the HO state and its associated phases in other materials.

DOI: 10.1103/RevModPhys.83.1301 PACS numbers: 71.27.+a, 74.70.Tx, 75.30.Mb

CONTENTS

I. HISTORICAL BACKGROUND

Uranium is an intriguing element, not only in itself but also as a basis for forming a variety of compounds and alloys with unconventional or puzzling physics properties (for recent reviews, see Sechovský and Havela, 1998, Santini, Lémanski, and Erdös, 1999, Stewart, 2006). Natural or depleted uranium, i.e., containing 99.5% ^{238}U, has a mild α radioactivity of 25 kBq/g, which allows U-based samples to be fabricated and studied in university laboratories with a minimum of safety precautions. Following the initial discoveries of unexpected superconductivity and heavy-fermion behavior in uranium-based compounds such as UBe_{13} (Ott *et al.*, 1983) and UPt_3 (Stewart *et al.*, 1984), it has become popular to synthesize uranium compounds and cool them in search of exotic ground states. Over the past 50 or so years many conducting and insulating systems have been synthesized, analyzed, and structurally characterized (Sechovský and Havela, 1998; Stewart, 2001, 2006). The usual classification of the metallic samples at low temperature is superconducting and/or magnetic, with some of the modern compounds designated as "exotic" (Pfleiderer, 2009).

Why are uranium-based materials so interesting? The observed variety of unusual behaviors derive directly from the U open $5f$ shell. Several defining electronic structure quantities of the U f electrons are all on the same energy scale: the exchange interaction, the $5f$ bandwidth, the spin-orbit interaction, and the intra-atomic f-f Coulomb interaction. As consequences, (i) elemental uranium displays intermediate behavior between the transition metals and the rare earths in their characteristic bandwidths, yet it generates the largest spin-orbit coupling; (ii) U lies directly on the border between localized and itinerant (or overlapping) $5f$ wave functions; (iii) the Wigner-Seitz radii R_{WS} of comparative elements place U near the minimum between metallic and atomic $5f$ wave functions; and (iv) ionic U can adopt six different valences when combined with other elements; usually one finds U^{4+} with two $5f$ electrons or U^{3+} with three $5f$ electrons. However, it is difficult to distinguish or separate these two valences in metallic systems with strongly hybridized f states which will then play a major role in the ground state properties. So we now have available a weakly radioactive element that can be tuned into unique chemical and electronic states thereby producing its exotic low-temperature behavior. Unfortunately a move to the right along the actinide series involves strong radioactive emissions, making low-temperature physical studies prohibitive except at specially equipped central facilities. The R_{WS} of elemental uranium overlaps with that of hafnium and is far away from the nearly constant R_{WS} of the rare earths. Yet Hf is more a superconducting

*mydosh@physics.leidenuniv.nl
†peter.oppeneer@physics.uu.se

basis than a magnetic one, while U sits on the "fence" between superconductivity and magnetism (Smith and Kmetko, 1983). For a historical review of the actinides, see Moore and van der Laan (2009).

As a traditional way of comparing the various U-based compounds the now-famous Hill plot (Hill, 1970) is most useful. Here one plots the ordering temperature (magnetic and/or superconducting) against the nearest-neighbor U-U spacings. According to the trends shown in Fig. 1, for small U-U distances superconducting compounds should be prominent. In the opposite limit, at large spacings greater than 3.5 Å, significant magnetic transitions are found. The position of URu_2Si_2 has been added in Fig. 1, where the superconducting and hidden-order transitions span the superconducting or magnetic line. Many of the exotic or strongly correlated intermetallic compounds, e.g., UBe_{13} and UPt_3, do not obey Hill's rule due to their strong hybridization of the $5f$ electrons with the conduction electrons regardless of the U-U overlap.

Among the exotic U-based compounds there are nine unconventional superconductors that combine superconductivity with magnetism (ferromagnetism and antiferromagnetism) or nearly magnetic behaviors (spin fluctuations, small moments, or enhanced susceptibility). For such systems the appellation "heavy fermion" has been applied along with "non-Fermi liquid" to describe their deviant behavior. Table III in Pfleiderer (2009) surveys these materials, among which UBe_{13}, UPt_3, and URu_2Si_2 are the most perplexing. From this table we can discern that magnetism plays a major role in the superconductivity, sometimes generating it, sometimes destroying it as we will see below. Here we have a comparison of these different materials which have been the subject of considerable research since the early 1980s (Pfleiderer, 2009).

II. INTRODUCTION TO URu_2Si_2

Only for one system, viz., URu_2Si_2, has there been continuing and intense interest for the past 25 years. In 1984 a poster by Schlabitz *et al.* (unpublished) was presented at a fluctuating-valence conference in Cologne showing the appearance of two transitions: one superconducting, and the other antiferromagnetic. There was no publication of these results (Schlabitz *et al.*, 1986) until after two Letter publications appeared in 1985 (Palstra *et al.*, 1985) and 1986 (Maple *et al.*, 1986). While all three groups agreed on the bulk superconductivity at ≈ 1.0 K, there were different interpretations for the magnetic transition at 17.5 K. Palstra *et al.* (1985) designated it a weak type of itinerant antiferromagnetism, Maple *et al.* (1986) a static charge-density wave (CDW) or spin-density wave (SDW) transition, and Schlabitz *et al.* (1986) a local U-moment antiferromagnet. We now know after 25 years that all three interpretations were incorrect. The transition at 17.5 K is not due to long-range-ordered magnetism and there is no measurable lattice modulation relating to a static CDW or SDW formation. Since the origin of the transition is unknown without a definite order parameter (OP) established for the emerging phase or for its characteristic elementary excitations, the term hidden order (HO) was adapted later on for the mysterious phase appearing at $T_o = 17.5$ K. Figure 2 illustrates the two dramatic, mean-field-like phase transitions in the specific heat. Note the large amount of entropy forming at T_o. The entropy $S = \int_0^{T_o}(\Delta C/T)dT$ is approximately $0.2R\ln 2$ (R being the gas constant), and, if the compound were magnetic, this result would indicate a large contribution that should be detectable with magnetic neutron scattering.

The dc magnetic susceptibility $\chi = M/H$ with $H = 2$ T is displayed in Fig. 3 for applied fields along the a and c axes.

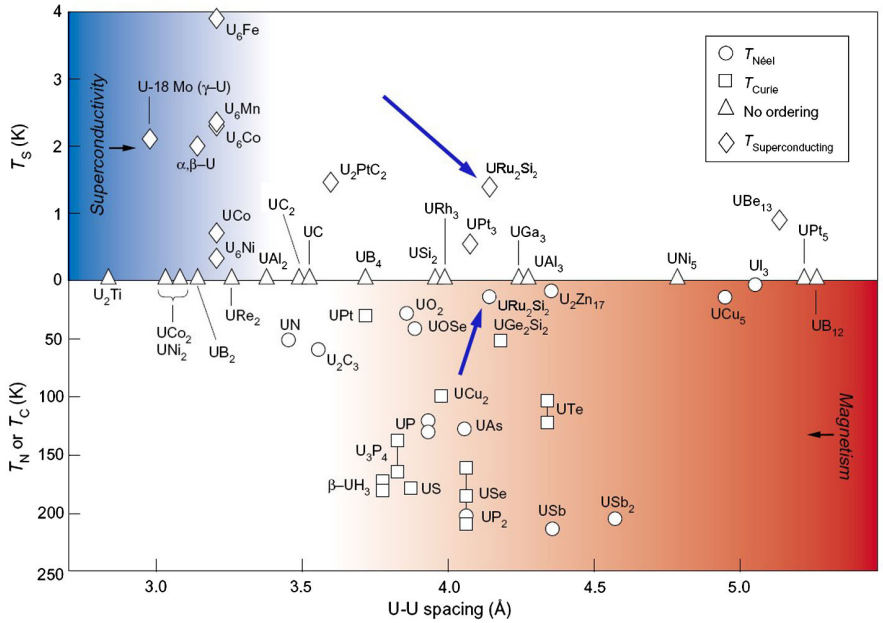

FIG. 1 (color online). The Hill plot for various uranium-based intermetallic compounds. The bottom arrow indicates the hidden-order transition temperature T_o of URu_2Si_2, while the top one indicates its superconducting transition temperature T_c. From Janik, 2008 and Moore and van der Laan, 2009.

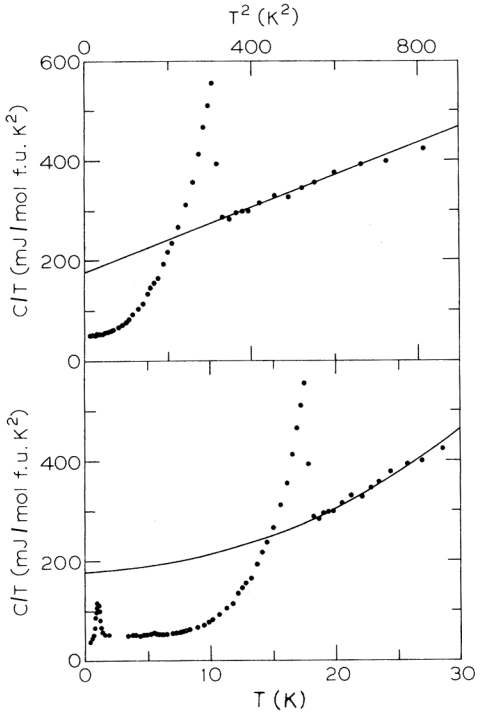

FIG. 2. Specific heat as a function of temperature for URu_2Si_2. Top: C/T vs T^2; bottom: C/T vs T with the superconducting transition also shown. Note the large extrapolated specific-heat coefficient γ of 180 mJ/mole K^2. From Palstra *et al.*, 1985.

The magnetic response is strongly Ising like, as there is a magnetic signal only along c which begins to deviate from a local-moment Curie-Weiss dependence below 150 K. The χ maximum at ≈ 60 K indicates the coherence temperature T^* and the formation of a heavy Fermi liquid. The HO transition is hardly seen but it corresponds to the intersection of the drop with the plateau below 20 K [cf. Pfleiderer, Mydosh, and Vojta (2006)]. Clearly the susceptibility of URu_2Si_2 is not that of a conventional bulk antiferromagnet. Nevertheless, there are several uranium compounds that do show a similar Ising-like behavior, for example, URhAl and UCo_2Si_2 [see, e.g., Sechovský and Havela (1998) and Mihalik *et al.* (2006)].

Although the HO transition always occurs at 17.5 K and is robust, not dependent on sample quality, the low-temperature properties are indeed sample dependent. In particular, the resistivity $\rho(T)$ exhibits stronger decreases as the purity of the starting U material is increased. A characteristic plot of $\rho(T)$ for the two a and c directions in the body-centered tetragonal (bct) unit cell of URu_2Si_2 (see below) is shown in Fig. 4. There is a negative temperature coefficient $d\rho/dT$ at high temperatures, followed by a maximum at ≈ 75 K, signaling the onset of lattice coherence, and then a dramatic drop to low temperatures and superconductivity. Presently one can find resistivity ratios of 500 or more in the best of today's samples. The explanation of the high-temperature resistivity ($T \gtrsim 100$ K) reaching $\approx 500\ \mu\Omega$ cm is open: either a strong Kondo-like scattering of incoherent, atomic U spins takes place or, since the resistivity is above the Joffe-Regel limit $k_F\ell \simeq 1$ (the product of the Fermi momentum and the mean free path), variable range hopping occurs. As the local U spins disappear with the onset of coherence when the temperature is lowered and the heavy-fermion state is created, the spin (fluctuation) scattering is removed and a coherent low-carrier state without significant scattering is formed. The superconducting transition temperature T_c varies significantly (between 0.8 and 1.5 K) with sample quality and purity and appears to coexist on a microscopic scale with the HO without disturbing it (Broholm *et al.*, 1987; Isaacs *et al.*, 1990).

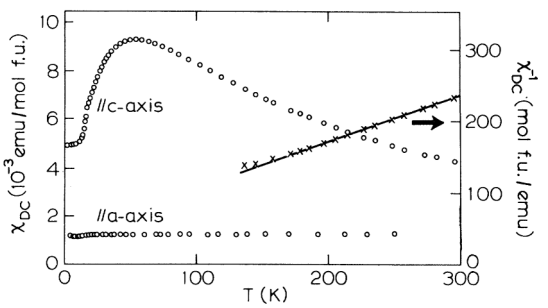

FIG. 3. Susceptibility χ of URu_2Si_2 with applied field (2 T) along the a and c axes. Note the deviation from the Curie-Weiss law ($\mu_{\rm eff} = 3.5\mu_B$/U; $\theta_{\rm CW} = -65$ K) along the c axis below 150 K. From Palstra *et al.*, 1985.

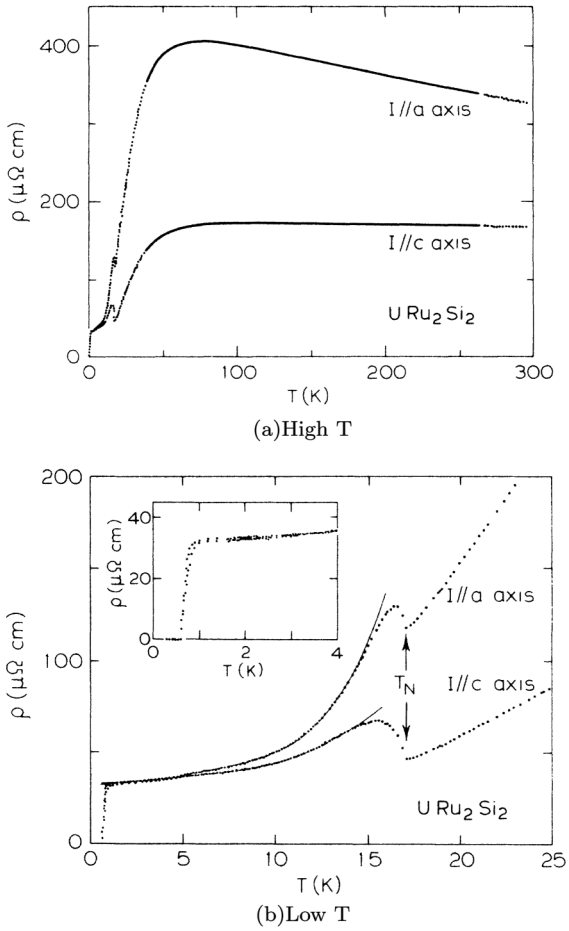

FIG. 4. Top: Overview of the resistivity ρ along the a and c axes. Bottom: Expanded view of the low-temperature resistivity illustrating the HO transition ($T_o = 17.5$ K) and the superconducting one ($T_c = 0.8$ K). From Palstra, Menovsky, and Mydosh, 1986.

Transport and thermodynamic measurements indicated a considerable Fermi-surface (FS) reconstruction occurring at the HO transition (Palstra *et al.*, 1985; Maple *et al.*, 1986). The measured electronic specific heat in the HO state and the jump in the resistivity at the transition are consistent with the opening of an energy gap over a substantial part of the FS. Maple *et al.* (1986) and Fisher *et al.* (1990) showed that the electronic specific heat in the HO state can be extremely well described by $C_e(T) \propto \exp(-\Delta/k_B T)$, where Δ is the charge gap opening in the electronic spectrum below T_o. Fits to the measured C/T data gave $\Delta \approx 11$ meV, and it was deduced that the gap opened over about 40% of the FS (Palstra *et al.*, 1985; Maple *et al.*, 1986). Subsequent resistivity (McElfresh *et al.*, 1987) and Hall effect measurements (Schoenes *et al.*, 1987) provided additional information on the opening of a gap at the HO transition. McElfresh *et al.* (1987) deduced from resistivity measurements a gap of about 7 meV, which with hydrostatic pressure increased to about 10 meV. The early Hall effect experiments of Schoenes *et al.* (1987) clearly evidenced the opening of a gap in the HO, accompanied by a remarkable drop in the carrier concentration. These measurements also provided a rough estimate for the single-ion Kondo temperature $T_K \approx 370$ K.

Thermal expansion experiments, $\alpha = L^{-1}(\Delta L/\Delta T)$, track the sample length L and hence the lattice constants a and c as a function of temperature surrounding the HO transition. The thermal expansion coefficient exhibits a large in-plane positive peak contrasting with the smaller negative one along the c axis, both sharply peaked at T_o (de Visser *et al.*, 1986). Hence, there is a net volume increase indicating a significant coupling of the HO to the lattice.

Because of the conjectures of the appearance of magnetism or a CDW at the HO transition, neutron scattering (Broholm *et al.*, 1987, 1991; Mason *et al.*, 1990) and x-ray magnetic scattering (Isaacs *et al.*, 1990) were brought to bear on the transition. By searching for scattering in directions where Bragg peaks were traditionally found in other compounds having the same $ThCr_2Si_2$ crystal structure with known long-range magnetic order, type-I antiferromagnetism was observed, with ferromagnetic a-a planes, alternating antiferromagnetically along the c direction (Broholm *et al.*, 1987, 1991; Isaacs *et al.*, 1990). Figure 5 illustrates the bct $ThCr_2Si_2$ structure (space group $I4/mmm$) along with the putative antiferromagnetic type-I magnetic order on the U sublattice. Although magnetic Bragg peaks were found at the proper $\mathbf{Q}$ values corresponding to the expected structure, there were particular difficulties with interpreting the neutron diffraction and x-ray Bragg peaks as conventional ordered-moment antiferromagnetism. (i) The magnetic Bragg-peak intensities were surprisingly small, corresponding to an ordered U moment of only $\mu_{\rm ord} \approx (0.04 \pm 0.01)\mu_B$/U (neutrons) and $\mu_{\rm ord} \approx (0.02 \pm 0.01)\mu_B$/U (x rays). Muon spin rotation (μSR) measurements provided an ordered moment that was even an order of magnitude smaller (MacLaughlin *et al.*, 1988). (ii) The magnetic correlation lengths of about 400 Å are not resolution limited, i.e., the magnetic order is not truly long ranged. (iii) The measured temperature dependence of the neutron and Bragg intensities does not resemble a typical order parameter curve with its convex T behavior. And (iv) there are strong sample-to-sample variations of the Bragg peaks, when their different temperature dependencies below T_o are compared. So although the conventional wisdom proposed a Néel-type magnetic explanation, even then (around 1990) there were serious qualms about such a mundane interpretation.

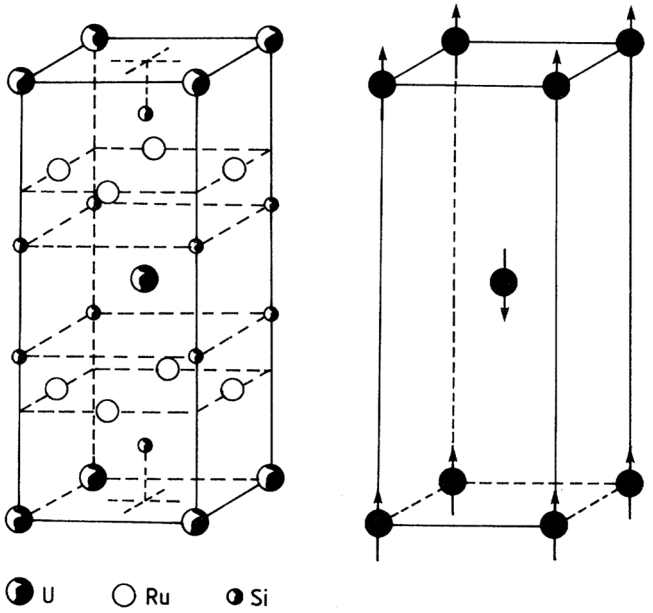

FIG. 5. Left: Crystal structure of body-centered-tetragonal URu_2Si_2 (space group: $I4/mmm$; lattice constants at 4.2 K $a = 4.124$ Å and $c = 9.582$ Å after a 0.1% contraction from 300 K). Right: The type-I antiferromagnetic c-axis spin alignment of U moments.

Early inelastic neutron work drew particular attention to magnetic excitations appearing at low temperatures, which revealed that the inelastic neutron response of URu_2Si_2 differed markedly from that of, e.g., UBe_{13} and UPt_3 (Walter *et al.*, 1986). Detailed neutron experiments were performed by Broholm *et al.* (1991) to detect the excitations or inelastic modes. They observed a continuous magnetic excitation spectrum, with two distinct gapped modes appearing at the antiferromagnetic wave vector $\mathbf{Q}_0 = (0, 0, 1)$ [equivalent to $(1, 0, 0)$] and at $\mathbf{Q}_1 = (1 \pm 0.4, 0, 0)$. Figure 6 shows the magnon energy-momentum dispersion determined by Broholm *et al.* (1991) overlaid with a full inelastic energy-momentum scan measured recently (Wiebe *et al.*, 2007; Janik *et al.*, 2009). The modes at (0, 0, 1) and (1.4, 0, 0) are commensurate and incommensurate, respectively, with the lattice. They sharply form at $T \lesssim T_o$ with gaps of about 2 to 4.5 meV, but, since the antiferromagnetic interpretation still prevailed in the early 1990s, they were designated as ordinary magnon modes (Broholm *et al.*, 1991). It was noted, though, that the antiferromagnetic mode was longitudinal and not transverse as is commonly expected for low-energy spin fluctuations. Thus the full meaning of these inelastic modes in the HO state was a mystery and these modes are of intense attention today both experimentally and theoretically. Are they the elementary excitations of the HO state that cause this spin gapping? See Sec. IV.

In order to determine the conductivity of URu_2Si_2 via a spectroscopic probe, the far-infrared reflectance was measured by Bonn, Garrett, and Timusk (1988) as a function of

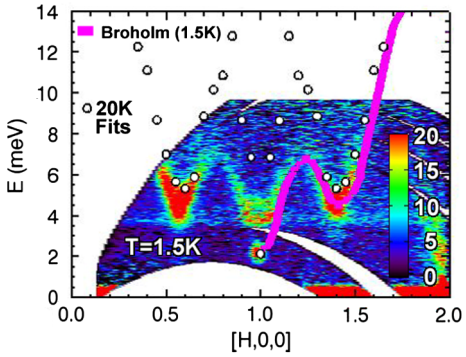

FIG. 6 (color online). Energy-momentum scan of spin excitations determined by inelastic neutron scattering at 1.5 K (Wiebe *et al.*, 2007). The color bar denotes the intensity of the modes. The two intense modes appear at $\mathbf{Q}_0 = (1, 0, 0)$ and $\mathbf{Q}_1 = (1 \pm 0.4, 0, 0)$ [note that the mode at $(1, 0, 0)$ is partially shaded by the equipment]. The curve gives the magnon dispersion determined by Broholm *et al.* (1991). Note also the commensurate gap at $\mathbf{Q}_0 = (1, 0, 0)$ and the larger incommensutate gap at $\mathbf{Q}_1 = (1 \pm 0.4, 0, 0)$. The **Q**-independent intensity detected at 3.9 meV is not due to a crystal electrical field excitation, but due to fission processes of ^{235}U. From Janik *et al.*, 2009.

frequency and temperature. Using an extended Drude model they tracked the optical conductivity into the coherence or heavy-fermion regime, characterized by reduced scattering and enhanced effective mass, and further down below T_o where a partial charge gap opens. This result confirms that the FS is being reconstructed in the transition to the HO state. Hence, combining transport, thermodynamic, and optical data with those obtained from inelastic neutron scattering, it is evident that the HO state possesses both a spin and a charge gap. Here we have the first clues about the microscopic HO behavior.

The enigmatic nature of the HO state first became recognized in the early 1990s. The magnetic entropy $S_m(T)$ of URu_2Si_2 had been determined from the λ-type anomaly observed in the specific heat (see Fig. 2) (Palstra *et al.*, 1985; Maple *et al.*, 1986; Schlabitz *et al.*, 1986), using $S_m(T) = \int_0^T (\Delta C/T')dT'$, where $\Delta C/T$ was obtained through subtracting the measured specific heat of $ThRu_2Si_2$, which has no $5f$ electrons, from that of URu_2Si_2. The entropy formed at T_o was determined to be about $0.2R\ln 2$, a relatively large value (Maple *et al.*, 1986; Schlabitz *et al.*, 1986; Fisher *et al.*, 1990). The magnetic entropy can be expressed as $R\ln(2S + 1)$, or as $R\ln 2$, assuming that N uranium atoms have an $S = 1/2$ spin, i.e., a $1\mu_B$ moment. It was noted that such a relatively large entropy change cannot, in particular, be explained by assuming an antiferromagnetically ordered phase with small moments of only $0.04\mu_B$ [see, e.g., Gor'kov and Sokol (1992), Ramirez *et al.* (1992), and Walker *et al.* (1993)]. Consequently, the detected small-moment antiferromagnetism (SMAF) failed to account for the phase transition, and another, hidden order was responsible.

During the last two decades a quest to uncover the HO arose. In these decades significant progress has been made in sample preparation and characterization. Superclean URu_2Si_2 samples were synthesized as well as samples with precisely controlled chemical substitutions. A wide variety of experimental probes were unleashed on the HO problem. Although our understanding about the HO has definitely increased, the nature of the HO has thus far proved elusive. Concomitantly, many exotic theoretical models were proposed to explain the HO. Some of these could be dismissed while for others even the experimental techniques to verify or falsify them do not yet exist. Nonetheless, the most recent experiments provided more and clearer constraints for the theories, whereby the multitude of mechanisms put forth for the HO could be narrowed down. Also, throughout these years, 1990–2010, significant progress was made in characterizing the unconventional superconducting properties through a variety of experimental probes. Experiments were carried out under pressure and with various dopings, both of which destroyed the HO and superconducting phases. The results of these studies have been summarized by Pfleiderer (2009), where the recent references are included.

III. WHAT IS HIDDEN ORDER?

Hidden order evolves as a clear phase transition to a new phase at temperature T_o as determined from bulk thermodynamic and transport measurements. The order parameter and elementary excitations of the new ordered phase are unknown, i.e., they cannot be determined from microscopic experiments. In URu_2Si_2 all bulk quantities show a mean-field-like (second-order) phase transition at 17.5 K, yet neutron and x-ray scattering, nuclear magnetic and quadrupole resonance (NMR, NQR), μSR, etc., are not able to reveal the OP and elementary excitations. We might mention four previous cases where the OP and elementary excitations were only uncovered many years after the experimental discovery: superconductivity, antiferromagnetism, 2D X-Y magnets, and spin glass.

Basic properties of the HO state in URu_2Si_2 are (i) the large reduction of entropy upon entering it, (ii) the opening of charge and spin gaps, (iii) a large decrease in the scattering rate along with a smaller effective mass, (iv) greatly reduced carrier concentration, (v) a clear coupling to the lattice, and (vi) an electronically ordered state that can be destroyed by pressure, magnetic field, and Rh doping. A highly unconventional (d-wave, even parity, spin-singlet) multigap superconducting ground state with $T_c \approx 1.5$ K evolves only out of the HO state (Kohori, Matsuda, and Kohara, 1996; Matsuda, Kohori, and Kohara, 1996). This has been the focus of recent investigations (Kasahara *et al.*, 2007, 2009; Matsuda *et al.*, 2008; Okazaki *et al.*, 2008; Yano *et al.*, 2008; Morales and Escudero, 2009).

Now the question arises: Is the HO phase generic, i.e., can it, as defined above, be found in other materials with different types of interactions? And then, once defined as HO, can it be unmasked and explained by known physical concepts and mechanisms? At present there is no comprehensive understanding of generic hidden order and its relation to quantum criticality. Nevertheless, the concept of HO is beginning to make headway into the recent literature. For example, in the overview article of Coleman and Schofield (2005) it was invoked as masking the quantum phase transition in $Sr_2Ru_3O_7$, where a putative nematic phase replaces the HO one. Recently the terms HO and unidentified low-energy

excitations were applied to the long-standing puzzle of the low-temperature phase transition in NpO_2 (Santini *et al.*, 2006). In this case the "unmasking" of the HO was the identification of a staggered alignment of magnetic multipoles. Long-range ordering of electric or magnetic multipoles has to date been unambiguously detected only in a few materials, with NpO_2, UPd_3, and $Ce_{1-x}La_xB_6$ being the most prominent examples. A review of HO as a higher-rank multipolar (nondipolar) driven phase transition is given by Kuramoto, Kusunose, and Kiss (2009) and Santini *et al.* (2009). A similar analogy can be drawn for the skutterudites, e.g., $PrFe_4P_{12}$ and $PrOs_4Sb_{12}$, where again a HO phase transition can be related to multipolar (quadrupolar) ordering and compared to URu_2Si_2 (Hassinger, Derr *et al.*, 2008; Sato, 2008). In addition, Dalla Torre, Berg, and Altman (2006) used HO to describe an unknown phase in a 1D Bose insulator which exists between the Mott and density wave phases, and Xu *et al.* (2007) used it for unidentified phases in a quantum spin fluid. High-temperature superconductors represent another area in which to look for HO (Valla *et al.*, 2006). Here the nature of the pseudogap phase in the high-temperature cuprates has persisted as a major unsolved problem. Recent experiments have attempted to expose its "hidden order" (He *et al.*, 2011). Finally, HO remains a possibility in the Ce-115 compounds (hidden magnetic order), the heavy fermions UBe_{13} and UPt_3, various organic charge-transfer salts near the metal-insulator transition, and nonmagnetic or nearly magnetic oxides (Manna *et al.*, 2010).

The term "hidden-order parameters" was apparently first used in 1996 by Buyers who was then casting doubt on the idea that the measured small magnetic dipole transition was truly intrinsic and that conventional antiferromagnetism was the mediator of the phase transition at 17.5 K. Buyers additionally noted that inelastic neutron modes (spin excitations) were strongly involved in the HO transition. As $T \rightarrow T_o$ from below, the $\mathbf{Q}_0 = (0, 0, 1)$ mode softens and its damping increases, thereby ruling out a crystal electric field (CEF) origin.

Shah *et al.* (2000) introduced the HO parameter in a Landau-Ginzburg free energy expansion which tried to describe the HO phase transition via two interacting order parameters, Ψ, the primary unknown OP of the HO state, and m, the magnetization as determined from neutron scattering and diffraction, as a secondary OP. Using such expansions Shah *et al.* (2000) were able to predict the magnetic-field dependence of both Ψ and m and thereby determine the symmetry of the coupling between the two order parameters $g\Psi \cdot m$ (bilinear) or $g\Psi^2 \cdot m^2$ (biquadratic).

These two scenarios were proposed for the two types of coupling posing the question: Does the Ψ order parameter break time-reversal symmetry or not? The latter is possible, e.g., if Ψ is related to a staggered electric quadrupolar order. Based upon the measured magnetic-field dependence of the neutron moment (Bourdarot *et al.*, 2003a, 2003b, 2005), the comparison favored the linear coupling scheme, thereby indicating that Ψ breaks time-reversal symmetry. Consequently the HO would have a limiting constraint in its specific representation (Shah *et al.*, 2000). However, while this deduction was sound the question still remained: Is the small magnetic moment m tracked by the neutron scattering

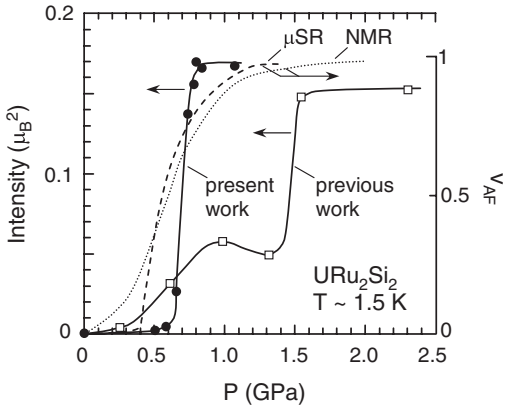

FIG. 7. Influence of the crystal purity on the phase separation between the HO and LMAF phases of URu_2Si_2. Shown is the pressure dependence of the integrated intensity of the $\mathbf{Q}_0 = (1, 0, 0)$ antiferromagnetic Bragg peak measured at 1.5 K for newer high-purity single crystals (closed circles) and older single crystals (open squares, data from Amitsuka *et al.*, 1999). Also shown is the pressure dependence of the antiferromagnetic volume fraction (right ordinate) derived from earlier ^{29}Si NMR (Matsuda *et al.*, 2001) and μSR (Matsuda *et al.*, 2001) measurements. A clear phase transition between the HO and antiferromagnetically ordered phases is present in the purer single crystals. From Amitsuka *et al.*, 2007.

intrinsic to the HO? This conundrum plagued the field for many years and it became a point of contention and dispute. Only in recent years has it been fully clarified that the small antiferromagnetic moment is extrinsic, i.e., likely related to defects and stress in the sample. Early μSR measurements provided evidence for the existence of spatially inhomogeneous HO regions and antiferromagnetic ones; the latter occupied about 10% of the sample volume (Luke *et al.*, 1994). Detailed ^{29}Si NMR studies (see below) supplied definite evidence for a spatially inhomogeneous development of antiferromagnetic regions with large moments of about $0.3\mu_B$ (Matsuda *et al.*, 2001). Further arguments against a homogeneous SMAF phase were derived from dilatation experiments (Motoyama, Nishioka, and Sato, 2003), μSR (Amato *et al.*, 2004), and recently, neutron Larmor diffraction (Niklowitz *et al.*, 2010). The small staggered moment of the putative SMAF phase originates thus from the smallness of the antiferromagnetic volume fraction, a scenario that was demonstrated by the fabrication of high-purity single crystals. In these high-quality samples the value of the detected small antiferromagnetic moment was reduced to $0.01\mu_B$, and a clear phase boundary between the HO and an ordered large-moment antiferromagnetic (LMAF) phase was observed (Amitsuka *et al.*, 2007). Figure 7 compares the pressure dependence of the antiferromagnetic Bragg peak at $\mathbf{Q}_0 = (1, 0, 0)$ for a high-purity single crystal ("present work") with data obtained on older single crystals ("previous work") (Amitsuka *et al.*, 2007).

IV. EXPERIMENTAL SURVEY

In 1999 Amitsuka *et al.* investigated the pressure dependence of the neutron magnetic Bragg peaks representing the SMAF, with $\mu_{\text{ord}} \approx 0.03\mu_B$. Previous bulk resistivity measurements at pressures up to 1.5 GPa had shown little

or no change in $\rho(T)$ or $d\rho/dT$ upon entering the HO phase. McElfresh *et al.* (1987) found only a slight increase of T_o as well as an increase of the transport gap. Surprisingly the Bragg-peak intensity at $\mathbf{Q}_0 = (1, 0, 0)$ exhibited a dramatic upturn at a pressure of 0.5 GPa. The corresponding ordered moment was $0.4\mu_B$, a change of almost 15 (see Fig. 7). This reasonably large U moment for a heavy-fermion material designated pressurized URu_2Si_2 as the expected LMAF with a conventional magnetic phase transition at $T_N \approx 18$ K. Figure 5 displays the LMAF spin order. The neutron experiments were followed by pressure-dependent ^{29}Si NMR probing the internal hyperfine fields in both the HO and LMAF states (Matsuda *et al.*, 2001, 2003). These found evidence for a phase separation in the HO state of a few volume percent LMAF, which increased with pressure, thereby giving the SMAF response. It is now generally accepted that puddles of the LMAF are generated by a stress field increasing the c/a axis ratio beyond a critical value (Yokoyama *et al.*, 2005). This extreme sensitivity to sample quality, e.g., stress, impurities, etc., has been emphasized by Matsuda *et al.* (2008) who compared resistivity and specific-heat data on samples cut from the middle with those on the surface of a high-quality single crystal. Figure 8 shows the most up-to-date measurements of the T-P phase diagram for URu_2Si_2 (Amitsuka *et al.*, 2007; Niklowitz *et al.*, 2010). Note the first-order phase transition separating the HO from the LMAF phase. Based upon the residual resistivity ratios a complete study of the crystal quality and various bulk properties has been carried out by Matsuda *et al.* (2011).

In order to probe the all-important Fermi surface in the HO phase of URu_2Si_2, quantum oscillations were studied, employing both de Haas–van Alphen (dHvA) and Shubnikov–de Haas (SdH) techniques (Ohkuni *et al.*, 1999; Nakashima *et al.*, 2003; Jo *et al.*, 2007; Shishido *et al.*, 2009; Hassinger *et al.*, 2010; Altarawneh *et al.*, 2011). The early angular-dependent dHvA measurements of Ohkuni *et al.* (1999) revealed three, rather small, closed FS pockets deep in the HO phase. This was once again consistent with a substantial FS gapping occurring in the HO phase. More recently, a

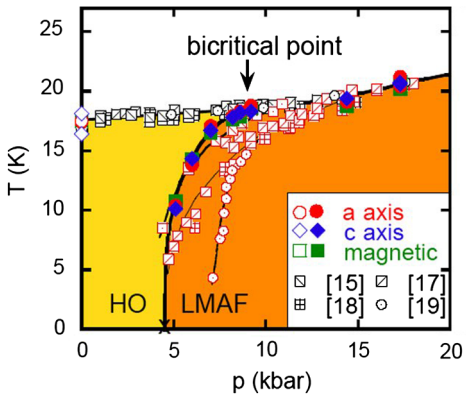

FIG. 8 (color online). Collection of the up-to-date experimental data representing the temperature-pressure phase diagram of URu_2Si_2 with HO and LMAF ordered states. The upper white region is the heavy Fermi (or Kondo) liquid out of which the HO and LMAF develop (Motoyama, Nishioka, and Sato, 2003; Amitsuka *et al.*, 2007; Hassinger, Knebel *et al.*, 2008; Motoyama *et al.*, 2008). From Niklowitz *et al.*, 2010.

larger, fourth FS sheet was found by SdH measurements on an ultraclean URu_2Si_2 sample (Shishido *et al.*, 2009). Up-to-date angle-dependent SdH measurements revealed a fifth branch, corresponding to a small FS pocket (Altarawneh *et al.*, 2011), as well as a previously unobserved splitting of one branch (Hassinger *et al.*, 2010); see Sec. VII. The quantum oscillation measurements performed by different groups provided data sets that are consistent with each other (cf. Hassinger *et al.*, 2010). Consequently, the FS of URu_2Si_2 in the HO has now definitely been established. The measured FS provides a stringent test for all theories of the HO. A full agreement with density-functional theory (DFT) calculations has only recently been achieved (Oppeneer *et al.*, 2010). An interesting ingredient for the HO puzzle has come from dHvA and SdH measurements under pressure, which allow one to probe the FS of the HO as well as of the LMAF phase. When pressure was applied to take the HO phase into the LMAF state, practically no change could be detected in the FS orbits as the pressure was increased to 1.5 GPa (Nakashima *et al.*, 2003; Hassinger *et al.*, 2010). The cyclotron effective mass decreased somewhat as expected for an increase in the magnetic moment. Accordingly, the FS with its partial gapping is not notably modified between the HO and LMAF phases. Consistent with this, the same FS nesting vector was detected by inelastic neutron experiments (Villaume *et al.*, 2008). Hence, the FSs of the HO and LMAF phases are similar, and furthermore these two distinct phases exhibit similar transport and thermodynamical properties. This behavior has been termed ''adiabatic continuity'' (Jo *et al.*, 2007), which, however, does not mean that these phases have identical OPs.

Since the quantum oscillations require a low temperature, usually tens of millikelvin, they cannot track the entrance into the HO phase at 17.5 K. This warrants a description of the high-temperature state out of which HO evolves. When the temperature is reduced below 100 K the incoherent local-moment-bearing U ions have long since disappeared due to their hybridization with the spd electrons of the ligands. Now a coherent heavy-fermion state is formed which in recent nomenclature is termed the heavy-electron Kondo liquid (KL) (Yang *et al.*, 2008). The characteristic KL temperature (coherence $T^\star$) is ≈ 70 K in URu_2Si_2 as determined from a variety of bulk measurements. By lowering the temperature below $T^\star$ a correlation or hybridization gap is expected to partially open at the FS due to f hybridization throughout this slow crossover into the KL. In heavy-fermion materials the KL should persist down to low temperatures (a few kelvins), where usually antiferromagnetic order or superconductivity occurs. However, in URu_2Si_2 already at 17.5 K the HO transition takes place with striking FS reconstruction and gapping.

Figure 9 collects three transport properties as the temperature is reduced from the paramagnetic KL through the HO into the superconducting state (Kasahara *et al.*, 2007). There is a continuous drop in the resistivity in the HO despite the loss of carriers as exemplified by the large jump in the Hall coefficient $R_H \propto 1/n$, the carrier concentration. Since $\rho = m^\star/(e^2 n\tau)$, the scattering rate $1/\tau$ must dramatically decrease to compensate for the reduction in n. Note the large residual resistivity ratio of 670 for the high-quality URu_2Si_2 crystal used. The effective mass $m^\star$ is not expected to vary

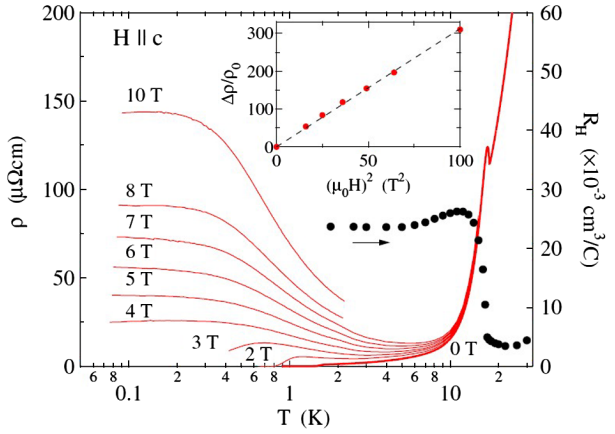

FIG. 9 (color online). Resistivity as a function of log$T$ in various magnetic fields (left scale). Hall coefficient through the HO transition (right scale). The inset shows the change of resistivity vs H^2. From Kasahara *et al.*, 2007.

significantly in this temperature region. The magnetoresistance $\Delta\rho(H)/\rho(0)$ is large and proportional to H^2, meaning that URu_2Si_2 is a compensated electron-hole semimetal, i.e., $n_e \approx n_h$ [as was noted originally by Ohkuni *et al.* (1999)]. Further analysis of the Hall data gives a hole concentration of ≈ 0.10 hole per U atom in the paramagnetic KL (Oh *et al.*, 2007) which becomes 0.02 hole per U atom in the HO (Kasahara *et al.*, 2007). It is remarkable that superconductivity can occur at such low carrier concentrations.

The thermal electricity of URu_2Si_2 is also unusual (Bel *et al.*, 2004). There are clear indications of the HO transition from the Seebeck coefficient (thermoelectric power) and an unusually giant Nernst effect (ratio of transverse electric field to longitudinal thermal gradient). These effects confirm the drastic decrease in the scattering rate and the low density of itinerant electrons that carry a large entropy.

Another transport property, the thermal heat conductivity κ, displays a steep increase when the HO state is entered from the KL (Behnia *et al.*, 2005; Sharma *et al.*, 2006). Since there are two contributions to κ one must separate the phonons (κ_p) from the electrons (κ_e). As the Wiedemann-Franz law is not fully valid here, the thermal Hall (or Righi-Leduc) conductivity κ_{xy} is used to independently determine κ_e. The electronic contribution is found to be extremely small with the phonons carrying most of the thermal conduction. This signifies the large FS gap opening at T_o which greatly decreases the electron-phonon scattering. By analyzing κ in terms of the mean-field Bardeen-Cooper-Schrieffer (BCS) model, one obtains a strong coupling of the HO with its itinerant electrons to the lattice, i.e., $2\Delta(T=0)/k_BT_o \approx 8$ (Sharma *et al.*, 2006). The applicability of an itinerant model to describe the κ data has been used to suggest a density wave scenario with strong lattice coupling (Sharma *et al.*, 2006). However, despite various attempts to find periodic lattice distortions, none have been detected. Solid-state probes that are sensitive to the local symmetry such as NMR and NQR would be able to detect these, but none have been found (Saitoh *et al.*, 2005).

The elastic properties of URu_2Si_2 have been measured with ultrasonic techniques (Wolf *et al.*, 1994; Kuwahara *et al.*, 1997). A softening is observed in the c_{11} and transversal $(c_{11}\text{-}c_{12})/2$ modes at temperatures below ~70 K, marking the onset of the coherence temperature (Kuwahara *et al.*, 1997). The elastic anomalies observed at T_o are in contrast quite small, indicating that no uniform distortion occurs at T_o. The longitudinal c_{11} shows a broad minimum at 30 K and increases slightly ($\sim 0.1\%$) when temperature is lowered (Wolf *et al.*, 1994; Kuwahara *et al.*, 1997).

Point-contact spectroscopy (PCS) measurements at temperatures around T_o have been applied to detect the opening of a conductance gap in the HO state (Hasselbach, Kirtley, and Lejay, 1992; Escudero, Morales, and Lejay, 1994; Thieme *et al.*, 1995; Rodrigo *et al.*, 1997; Morales and Escudero, 2009). All PCS data generally evidence the opening of such a gap; however, its onset is consistently found at about 19–25 K and not at T_o. As explained by Rodrigo *et al.* (1997), the pressure that is exerted to drive the point contact in the surface causes a local shift of T_o to a higher value. PCS measurements at higher temperature detected the onset of a resonance structure at the Fermi level starting at $T \approx 60$ K, consistent with the opening of a coherence or hybridization gap at $T^\star$ (≈ 70 K) derived from bulk Hall and resistivity measurements (Palstra, Menovsky, and Mydosh, 1986; Schoenes *et al.*, 1987). Morales and Escudero (2009) applied PCS to the superconducting state to probe the superconducting gap below $T_c = 1.5$ K. They observe this gap, but unexpectedly and unexplained, its temperature dependence does not follow a BCS-type shape and its onset starts above T_c.

Resistivity studies under pressure were performed by Jeffries *et al.* (2007, 2008), and Motoyama *et al.* (2008), who tracked the evolution of the charge gap from the HO into the LMAF phase. The transport gap was found to increase, when crossing from the HO to the LMAF, with the HO gap being about 70% to 80% of the LMAF gap. A kink in the critical temperature was also detected when passing from T_o to T_N under pressure.

Inelastic neutron-scattering (INS) redux was carried out by Wiebe *et al.* (2007) at temperatures spanning the HO transition. They tracked the commensurate $\mathbf{Q}_0 = (1, 0, 0)$ and incommensurate $\mathbf{Q}_1 = (1.4, 0, 0)$ modes to higher energies and temperature. The characteristic gap energies of 2 and 4 meV of these sharp spin waves were found in the HO phase. Above T_o the $\mathbf{Q}_0$ mode transforms to weak quasielastic spin fluctuations. In contrast, the $\mathbf{Q}_1$ mode is due to fast, itinerant-like, well-correlated spin excitations reaching energies up to 10 meV, i.e., a continuum of excitations. They relate these incommensurate spin fluctuations to the heavy quasiparticles that form below the coherence temperature $T^\star$ with a corresponding increase in entropy. The gapping of such strong spin fluctuations was related by Wiebe *et al.* (2007) to the loss of entropy at the HO transition. By analysis of the spectrum for $T > T_o$ the specific heat could be estimated, along with the entropy loss. The calculated relationship between the spin excitation gapping and the Fermi-surface gap establishes the strong coupling between spin and charge degrees of freedom for this collection of itinerant electrons. Therefore, the HO can be viewed as a rearrangement of electronic states at the Fermi energy, giving rise to the gapping of these two coupled but distinct types of excitations. Yet the mechanism of the HO or "driving force" causing the gapping and the electronic

rearrangement remain unknown (Wiebe *et al.*, 2007). As noted here, in accordance with earlier neutron studies, no CEF excitations were found up to 10 meV.

Further INS experiments examining the intriguing inelastic modes behavior were carried out in Grenoble (Villaume *et al.*, 2008). Here the pressure and temperature dependence of the $\mathbf{Q}_0$ commensurate mode was determined as the HO was entered from above. With pressure $\mathbf{Q}_0$ transforms from an inelastic excitation to a normal magnetic Bragg peak in the LMAF, i.e., the longitudinal spin fluctuations "freeze" and become static long-range antiferromagnetic order, with $\mu_{\mathrm{ord}} \approx 0.4\mu_B$. In contrast the incommensurate $\mathbf{Q}_1$ mode persists as inelastic to the highest pressures, with an increase in its energy. $\mathbf{Q}_1 = (1.4, 0, 0)$ represents thus a FS nesting vector found in both the HO and LMAF phases. Conversely, the antiferromagnetic mode at $\mathbf{Q}_0$ is a true signature of the HO (Villaume *et al.*, 2008). The T-P phase diagram extracted from the neutron scattering supplemented by thermal expansion and calorimetric data (Hassinger, Knebel *et al.*, 2008) is similar to that shown in Fig. 8. Hence, one can now follow the intensity of the antiferromagnetic spin fluctuations at $\mathbf{Q}_0$ out of the KL into the HO.

Recently a detailed study of the (polarized) inelastic neutron resonances at $\mathbf{Q}_0$ (and $\mathbf{Q}_1$) was performed by the Grenoble group, focusing on the commensurate antiferromagnetic resonance at (0, 0, 1) (Bourdarot *et al.*, 2010). The dynamical spin susceptibility $\chi(\mathbf{Q}, \omega, T)$, which is related to the spin-spin correlation function, was determined and analyzed above and below T_o. Clear spin correlations at $\mathbf{Q}_0$ were observed as the temperature was scanned through T_o with a jump in the resonance energy or spin-gap energy E_0 and a BCS-like T behavior of the integrated imaginary susceptibility; see Fig. 10. Elgazzar *et al.* (2009) predicted that the integrated spin-spin correlation function should display OP behavior. It thus appears that the $\mathbf{Q}_0$ spin resonance is a main signature of the HO phase. As proposed by Wiebe *et al.* (2007) the incommensurate $\mathbf{Q}_1$ mode that appears in both the HO and LMAF phases accounts for a large share of the loss of entropy due to gapping of the mode and corresponding loss of spin fluctuations. A major question is how the spin gap is connected to the charge gap of the FS. Is the spin resonance at the antiferromagnetic wave vector driven by the electronic gapping of the FS, or vice versa, is the spin resonance responsible for the FS gapping? In order to explain the observed behavior Bourdarot *et al.* (2010) suggested that both itinerant and local $5f$ electrons are playing a role, with itinerant electrons responsible for the spin gaps and localized electrons for the FS gap, thereby requiring a duality interpretation. Figure 11 collects the various energy scales for the neutron resonances and compares them with the gap energies from bulk resistivity measurements. Note the stepwise increase of the charge gap Δ_G at the HO-LMAF phase transition. The spin gap E_1 of the incommensurate mode also increases stepwise, whereas the commensurate mode with gap E_0 vanishes in the LMAF.

With this collection of sophisticated experiments on ever improving crystal quality, what have we learned about HO? We now give a brief summary to conclude this section.

HO is not a magnetic dipole (local-moment) ordered transition and ground state. Yet as with all strongly correlated

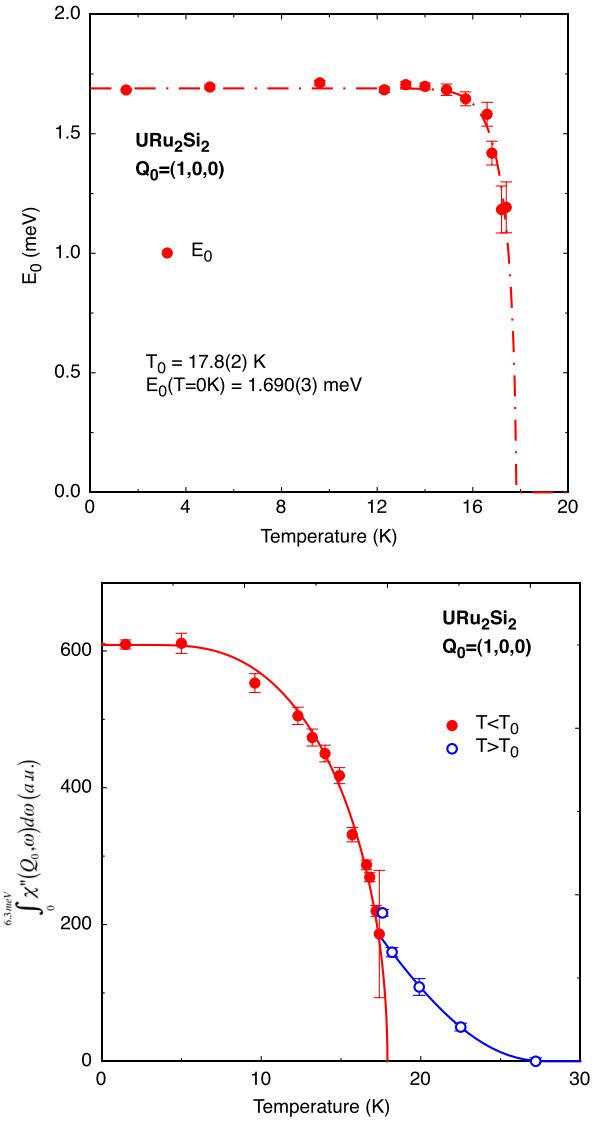

FIG. 10 (color online). Top: The gapping of the spin resonance at the antiferromagnetic wave vector, $\mathbf{Q}_0 = (1, 0, 0)$ vs temperature. Note the sudden onset of the spin gap E_0 upon entering the HO state. Bottom: The integrated dynamical spin susceptibility of the antiferromagnetic spin resonance vs temperature. The integrated intensity displays order parameter behavior and thus tracks the OP of the HO. From Bourdarot *et al.*, 2010.

electron systems magnetism hovers in the background, ever ready to make an appearance, in our case as dynamical spin excitations. The salient features of the HO are the pronounced Fermi-surface reconstruction and gapping at T_o. Surprisingly, there is practically no change in the FS properties between HO and LMAF phases. The high-T phase out of which HO appears can be designated as the recently proposed Kondo liquid (Yang *et al.*, 2008). This raises the question as to the exact nature of a Kondo effect in URu_2Si_2. Above T_o a correlation or hybridization gap slowly opens in the coherence crossover regime, but its importance has been neglected until now. The FS topology of URu_2Si_2 in the HO has now been determined to consist of only relatively small, closed pockets. The HO ground state is that of a low-carrier-concentration, compensated semimetal with strong lattice

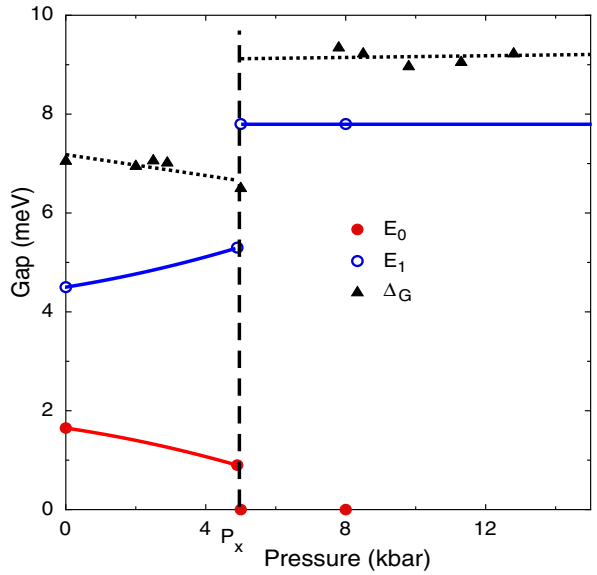

FIG. 11 (color online). Energy gap scales of HO and LMAF phases determined from INS resonances and bulk resistivity measurements as a function of pressure spanning HO to LMAF. Δ_G is the transport gap, whereas E_0 and E_1 are the gaps of the commensurate and incommensurate spin resonances, respectively. From Bourdarot *et al.*, 2010.

coupling. Itinerant electrons appear to be the main characters here as most experimental evidence supports an itinerant electron or bandlike scenario. There is no "smoking gun" for a localized uranium $5f^2$ or $5f^3$ configuration [see Oppeneer *et al.* (2010) for a discussion of this issue].

The INS has given us two modes or resonances: Preeminent is the $\mathbf{Q}_0$ commensurate resonance which mimics OP behavior of the HO state. The $\mathbf{Q}_1$ incommensurate spin mode, present in both the HO and LMAF phases, could be responsible for the similar loss of entropy at T_o in the HO and at T_N in the LMAF phase (Wiebe *et al.*, 2007; Balatsky *et al.*, 2009). There is an intimate relationship between charge and spin degrees of freedom. A special charge-spin duality or coupling seems to exist here analogous to that in the topological insulators, where a similar charge-spin duality comes into play (Hasan and Kane, 2010). Nevertheless, the driving force or mediator for creating the HO transition remains to be clarified.

V. THEORETICAL SURVEY

There have been a large number of theoretical contributions to the HO problem spanning the past 25 years. We review these here and attempt to relate them to the present experimental developments.

The earliest theoretical models focused on explaining the unusually small ordered moment and its Ising-like behavior that had been found in the neutron-scattering and susceptibility experiments (Palstra *et al.*, 1985; Broholm *et al.*, 1987). A first CEF model for URu_2Si_2 was developed by Nieuwenhuys (1987), who considered a U^{4+}-$5f^2$ ion with total angular momentum $J = 4$ in a tetragonal crystal field. He showed that a reasonable agreement with experimental susceptibility data could be obtained when the three lowest CEF levels were singlets with a splitting of about 40 K between the ground and first excited states [$|\Gamma_1^{(1)}\rangle = \alpha(|4\rangle + |-4\rangle) + \beta|0\rangle$ with $2\alpha^2 + \beta^2 = 1$ and $|\Gamma_2\rangle = (|4\rangle - |-4\rangle)/\sqrt{2}$, respectively]. The predicted ordered moment was, however, 10 times larger than the measured one.

Two early theoretical models began to treat the HO phase beyond the simple small-moment antiferromagnetic ordering. To explain non-Néel magnetically ordered phases characterized by weak antiferromagnetism, Gor'kov (1991) and Gor'kov and Sokol (1992) proposed double [$\langle S_\alpha(\boldsymbol{r}_1)S_\beta(\boldsymbol{r}_2)\rangle$] and triple [$\langle S_\alpha(\boldsymbol{r}_1)S_\beta(\boldsymbol{r}_2)S_\gamma(\boldsymbol{r}_3)\rangle$] spin correlators as driving order parameters which break spin rotational symmetry, while the local magnetization is zero. Here the spins can be on different U ions or on the same U ion, in which case the spin correlators are equivalent to quadrupole or octupole moments. Ramirez *et al.* (1992) analyzed the nonlinear susceptibility and proposed a double-spin correlator that would give rise to a staggered quadrupolar order.

Walker *et al.* (1993) performed angular-dependent *polarized* neutron scattering to search for higher-order spin correlators and spin nematic order parameters. A substantial neutron spin-flip scattering was observed, which was interpreted as evidence against a spin nematic or quadrupolar magnetization distribution. Various higher-order multipoles could be excluded as well. It is, however, a question as to how far these measurements were influenced by a parasitic SMAF phase. As a test of the proposed non-Néel orders, Barzykin and Gor'kov (1993) predicted that broken-symmetry Bragg peaks should exist for spin nematic and triple-spin correlator phases that could be induced with an external magnetic field. Neutron experiments searching for such a field dependence were undertaken but gave a null result, thereby causing these theories to be discarded (Mason *et al.*, 1995; Buyers, 1996).

An extensive CEF treatment was developed by Santini and Amoretti (1994), who considered the same U^{4+} CEF Hamiltonian as did Nieuwenhuys (1987), but analyzed in detail the possible energetic orderings of the nine CEF states and considered different angular momentum operators that can support multipolar order parameters. They observed that there exist three possible variants for the three lowest singlet levels. The first variant (A), which was considered by Nieuwenhuys (1987), could support dipole order (J_z) simultaneously with hexadecapole order [$J_xJ_y(J_x^2 - J_y^2)$], but this variant was rejected because it would give a much too high Schottky contribution to the specific heat. The other two variants (B and C) could both sustain a quadrupole (J_xJ_y or $J_x^2 - J_y^2$) and an octupole [$J_z(J_x^2 - J_y^2)$ or $J_zJ_xJ_y$] order parameter. Based on a comparison with experimental data, Santini and Amoretti (1994) favored electric quadrupolar ordering of localized f electrons for the HO. The dipole matrix elements would be zero for these two variants, but they suggested that a small static dipole magnetic moment could be induced by quadrupolar ordering. Walker and Buyers (1995), however, noted that dipole order cannot be induced as a secondary OP by quadrupolar order and that the proposal was not compatible with the polarized neutron scattering [see also Santini (1998) and Santini and Amoretti (1995)]. As mentioned before, there is to date no experimental evidence of such localized CEF levels and splittings.

A different CEF interpretation was proposed by Barzykin and Gor'kov (1995) who suggested that the U ion could be in an *intermediate valence* configuration, dominantly U^{4+}, but with a small admixture of half-integer spin configurations ($5f^1$ or $5f^3$) being responsible for the small moment.

The first suggestion of an itinerant-localized duality model was made by Sikkema *et al.* (1996), who developed an Ising-Kondo lattice model, in which they adopted the U^{4+} two-singlet CEF level ground state (variant A) with additional on-site exchange coupling to the conduction-electron spins, leading to Kondo screening. In this model the HO is explained as small-moment antiferromagnetism, but the appearance of such a state is now regarded as being parasitic to the HO. Another itinerant-localized duality model was suggested by Okuno and Miyake (1998). They used an induced-moment mechanism for the SMAF appearing from a singlet-singlet CEF scheme along with a partially nested FS of the itinerant electrons. Accordingly, the SMAF is found to be compatible with the large specific-heat jump and is composed of both spin and orbital components. While the duality model is also employed in more current HO theories [see, for example, Tripathi, Chandra, and Coleman (2005)], here it is focused on explaining the SMAF which is now believed to be extrinsic.

Kasuya (1997) proposed that the HO would be due to dimerization on the U sublattice. Here the corresponding atomic displacements should be observable with x-ray diffraction or extended x-ray absorption fine structure but have never been detected.

Another novel starting point for the HO transition is the unconventional SDW theory by Ikeda and Ohashi (1998). In this model the electron-hole pair amplitude changes its sign in momentum space. For the *d*-wave superconductors this is called a *d* density wave (DDW). Using a mean-field extended Hubbard model, the energy gap and thermodynamic properties can be calculated. They exhibit a sharp specific-heat cusp, a clear drop in the uniform susceptibility, and a zero staggered magnetization. Except for the susceptibility the above temperature dependence agrees with experimental results. However, a microscopic signature of the DDW has not yet been found. Presumably an angle-resolved photoemission spectroscopy (ARPES) measurement would be able to detect the FS modulation in k space. A modern extension of the DDW model is the chiral DDW of Kotetes and Varelogiannis (2010) and Kotetes, Aperis, and Varelogiannis (2010) who demonstrated that a chiral ground state could be responsible for the anomalous thermoelectric and thermomagnetic effects (e.g., the Nernst effect) in URu_2Si_2.

As mentioned above, different CEF schemes can be adopted for the U^{4+} ion. Experiments performed on diluted $U_xTh_{1-x}Ru_2Si_2$ with $x \leq 0.1$ (see below) were interpreted as an indication of a *doublet* CEF ground state (Amitsuka and Sakakibara, 1994). If the $5f^2$ CEF ground state is assumed to be a non-Kramers Γ_5 doublet ($|\Gamma_{5\pm}\rangle = \gamma|\pm 3\rangle + \delta|\mp 1\rangle$, $\gamma^2 + \delta^2 = 1$) in stoichiometric URu_2Si_2 as well, different multipole characters could become possible. Ohkawa and Shimizu (1999) considered the Γ_5 doublet and from a consideration of angular momentum matrix elements proposed that a magnetic dipole or a nonmagnetic quadrupole can be formed. Depending on the fine-tuning (e.g., pressure), one can transform one ground state into the other. So within this local CEF scheme the HO and the LMAF phases are explained as quadrupolar and spin-dipolar ordering, respectively. Once again, the local CEF levels have never been experimentally observed; they should be hybridized away in a KL. Yet, based upon an analysis of the dHvA amplitude (Ohkuni *et al.*, 1999) as a function of magnetic-field orientation, a series of 16 nodes appear. This behavior can be related to an Ising degree of freedom in the U^{4+} electronic configuration that would be possible with a Γ_5 doublet. According to Silhanek, Harrison *et al.* (2006) the local Γ_5 doublet becomes hybridized with the conduction electrons and itinerant quasiparticle bands having Γ_5 character are formed via this hybridization. This model then proposes itinerant antiferromagnetic quadrupolar order for the HO. Although such electrical quadrupoles could be detectable with resonant x-ray scattering (RXS) they have thus far not been observed (Amitsuka *et al.*, 2010; Walker *et al.*, 2011).

Yamagami and Hamada (2000) proposed that the HO could be an antiferromagnetic phase with a small magnetic moment caused by cancellation of a large spin and an equally large but antiparallel orbital moment. Neutron form factor measurements would be able to detect this, but could not confirm this effect [see, e.g., Broholm *et al.* (1991) and Kuwahara *et al.* (2006)].

Within the basic ingredients of a heavy Fermi liquid, Chandra *et al.* (2002) proposed that the HO in URu_2Si_2 resulted from *incommensurate* orbital antiferromagnetism associated with circulating charge currents between the U atoms. The model was based upon the appearance of a weak internal field below T_o detected by the ^{29}Si NMR linewidth broadening (Bernal *et al.*, 2001). These plaquette currents cause an orbital moment to form, thereby breaking time-reversal symmetry, which can be estimated from the isotropic field distribution at the Si sites. Thus the HO order parameter is taken to be proportional to the temperature onset of the linewidth broadening. Chandra *et al.* (2002) calculated the local fields and the large entropy transition in the specific heat, and detailed predictions were made to relate the incommensurate current ordering to the neutron-scattering cross section. A ring of scattering intensity was forecast at a specific anisotropic $\mathbf{Q}$ radius, which was experimentally sought but not found (Wiebe *et al.*, 2004). In addition, the NMR linewidth broadening was found to be much reduced when higher-quality stress-free single crystals were investigated (Bernal *et al.*, 2006; Takagi *et al.*, 2007).

Scenarios for higher-order multipolar transitions were put forward by Fazekas, Kiss, and Radnóczi (2005) and Kiss and Fazekas (2005). By assuming an itinerant to localized transition upon entering the HO phase from above, Kiss and Fazekas (2005) treated the HO state as having multipolar orders via symmetry-group theoretical arguments. Within the three-singlet CEF model, U^{4+} $5f^2$ ions can carry a sequence of higher-multipole order parameters. They considered a manifold of multipolar order parameters spanning the gamut from magnetic dipoles (rank 1) to magnetic triakontadipoles (rank 5). Led by the time-invariance breaking detected by neutrons (Walker *et al.*, 1993; Bourdarot *et al.*, 2003a), by NMR (Bernal *et al.*, 2001, 2006), and μSR (Amato *et al.*, 2004), they proposed staggered octupolar order for the HO,

which would be time-reversal-symmetry breaking and have a vanishing total dipolar moment. Further arguments were based on comparisons with uniaxial stress measurements, from which they concluded that a triakontadipole (which also breaks time-reversal symmetry) would be incompatible with the uniaxial response to stress. Notably, Fazekas, Kiss, and Radnóczi (2005) predicted the onset of octupolar order at T_o, followed by a second transition due to quadrupolar ordering at $T \approx 13.5$ K. While this theoretical conjecture is most intriguing, the observation of multipoles of rank higher than 2 is experimentally hardly accessible. Also, there is little evidence for another transition below T_o. Nevertheless, this work inspired a succession of additional theoretical efforts directed toward higher-order multipoles. Hanzawa and Watanabe (2005) adopted a singlet-doublet CEF level scheme and deduced that $J_x(J_y^2 - J_z^2)$ octupolar order would be most probable. Incommensurate ordering of octupoles was suggested by Hanzawa (2007). Recently, an antiferro ordering of time-even hexadecapoles was proposed as an HO parameter by Haule and Kotliar (2009), and a ferromagnetically aligned ($\mathbf{Q} = \mathbf{0}$) time-odd triakontadipolar HO parameter was proposed by Cricchio *et al.* (2009). Antiferro-quadrupole order of a J_xJ_y type was proposed by Harima, Miyake, and Flouquet (2010), and antiferro-hexadecapolar ordering of $xy(x^2\text{-}y^2)$ type was proposed by Kusunose and Harima (2011). A full review of multipole orders in strongly correlated electron systems was recently given by Kuramoto, Kusunose, and Kiss (2009) and Santini *et al.* (2009).

A serious drawback of the CEF multipolar theories is that these from the outset assume a localized $5f^2$ configuration, but as mentioned before, there is no experimental evidence for such localized CEF levels and splittings. Moreover, recent resonant x-ray scattering experiments sought for quadrupolar order but could not observe it (Amitsuka *et al.*, 2010; Walker *et al.*, 2011). This would thus exclude any quadrupole scenario. Also, as discussed by Walker *et al.* (2011) the magnetic form factor of URu_2Si_2 is normal, which would exclude magnetic octupolar and triakontadipolar orders. Conversely, previous RXS measurements on established multipolar ordered materials did, for example, unambiguously detect noncollinearly staggered quadrupole order in NpO_2, $Ce_{1-x}La_xB_6$, and UPd_3 [see Paixão *et al.* (2002), Walker *et al.* (2006), and discussions provided by Santini *et al.* (2009) and Kuramoto, Kusunose, and Kiss (2009)]. Also, NMR measurements have been shown to be able to detect quadrupolar symmetry breaking in NpO_2 [see, e.g., Tokunaga *et al.* (2005)], although it could be that contributions cancel out in URu_2Si_2. An often neglected aspect of CEF theories is that they do offer insight into the possible multipole symmetries on a single U ion, but this is not sufficient to achieve collective long-range order, which requires a mechanism providing an exchange coupling of multipoles. Investigations of the multipolar exchange interaction are only in their initial phase [cf. Suzuki, Magnani, and Oppeneer (2010)]. Last, while thus far all CEF theories assume a U^{4+} ion, a recent electron energy loss spectroscopy (EELS) study determined a $5f$ occupation of 2.7 (Jeffries *et al.*, 2010), which is not close to a $5f^2$ configuration. The EELS result, combined with a magnetic entropy approaching $S_{\mathrm{mag}} \sim R\ln 4$ at high temperatures (Janik, 2008), rather suggested that a Kramers $5f^3$ ion was realized at high enough temperatures. As mentioned before, at low temperatures an itinerant f character appears to prevail.

Helicity order, i.e., the establishment of a fixed axis of quantization for the spins on the FS, was proposed as the source of HO by Varma and Zhu (2006). Such order arises when the Pomeranchuk criteria for the spin-antisymmetric Landau parameters are violated with respect to the Fermi-liquid state. In order to remove or "cure" this instability, a nematic phase transition occurs, thereby creating the HO phase. For URu_2Si_2, this model represents a displacement of the FS into up and down sheets. Based upon the then-known band structure and FS, and variations of the density of states near the FS, Varma and Zhu (2006) calculated different experimental features: specific heat, linear and nonlinear susceptibilities, and the NMR linewidth broadening. Using the properly modified Landau parameters, good agreement with the data was found. The main difficulty with this approach is the neglect of the exact, complex FS and its significant hot spot gapping upon entering the HO state. Also, as spin-orbit coupling is strong in uranium, a picture of pure spin-up and spin-down states is not sufficient. Positron annihilation was employed to study FS changes in the HO, but could not confirm helicity order if this state forms as a single domain (Biasini, Rusz, and Mills, 2009). Up until now the suggested microscopic experimental verifications (Varma and Zhu, 2006) of the helicity order have not been accomplished.

By way of relating the HO transition to a SDW, Mineev and Zhitomirsky (2005) employed a double dual approach whereby two order parameters Ψ and m were considered. In addition, there were also two subsystems: local CEF moments on the U^{4+} sites along with conduction electrons in nested bands. Strong electron-electron interactions were added to drive the SDW in a commensurately nested FS. The SDW then induces a local SMAF or m in the HO state. Ψ represents the SDW amplitude and is the primary order parameter which governs the experimental behavior. The pressure dependence is predicted to show a line of first-order transitions ending in a critical end point that separates the SMAF from the LMAF. The high-magnetic-field properties are calculated from the model to account for the multiple phases (see Sec. VI). Unfortunately the experiment does not find a SDW even with a small form factor, and it is now commonly accepted that the SMAF is extrinsic, and instead of a critical end point there is the merging of all three phase lines at a bicritical point (Motoyama, Nishioka, and Sato, 2003; Amato *et al.*, 2004; Amitsuka *et al.*, 2007; Hassinger, Knebel *et al.*, 2008; Niklowitz *et al.*, 2010). Figure 8 presents the up-to-date pressure-temperature phase diagram for URu_2Si_2. Note the three distinct phases: KL, HO, and LMAF. The SMAF is omitted since it is extrinsic.

VI. HIGH MAGNETIC FIELDS AND Rh DOPING

There were various pioneering attempts to study the high-magnetic-field $\boldsymbol{H}$ behavior of URu_2Si_2 in the HO state and beyond by de Boer *et al.* (1986) and Sugiyama *et al.* (1990). Such experiments showed the destruction of the HO phase transition with fields approaching 35 T and the

occurrence of novel phases between 35 and 42 T. However, the use of short-time (< 1 ms) pulsed fields resulted in a loss of temperature equilibrium for these highly conducting samples and the T-H phase diagram was unclear. Here the field $\boldsymbol{H}$ is applied along the tetragonal c axis, with little or no magnetic response for fields in the basal plane.

More recent investigations began in 2002 with continuous H fields reaching 45 T for specific heat, the magnetocaloric effect (MCE), and magnetoresistance (Jaime *et al.*, 2002; J. S. Kim *et al.*, 2003). These measurements detected the suppression of the HO phase at 35.9 T (H_0), the appearance of a new phase between 36.1 T (H_1) and 39.7 T (H_2) with no additional phase transition above 40 T. While the low-field HO transition in the specific heat is λ like (second order), with increasing field its shape changes to a symmetric peak indicating a first-order transition. The new high-field phase is always reached through a first-order transition. The above results are confirmed via the MCE, which uncovers an increase in the magnetic entropy at H_0, a drop in S_{mag} at H_1, concluding with a final entropy rise above H_2. The magnetoresistance also established this three-step behavior.

Long-time pulsed (> 100 ms) magnetic fields were brought to bear for magnetization experiments reaching 44 T at 0.5 K (Harrison, Jaime, and Mydosh, 2003). These measurements revealed that the HO phase is destroyed before the appearance of the reentrant phase between 36 and 40 T. At temperatures above the maximum in the "novel" phase, ≈ 6 K, the magnetization and susceptibility (dM/dH) indicate an itinerant electron metamagnetism, i.e., an ever-sharpening peak in the susceptibility that disappears at the reentrant transition. Yet extrapolation of its T dependence through the novel phase suggests a quantum critical end point at 38 T. Thus, a putative quantum critical point is overpowered by the formation of the novel phase.

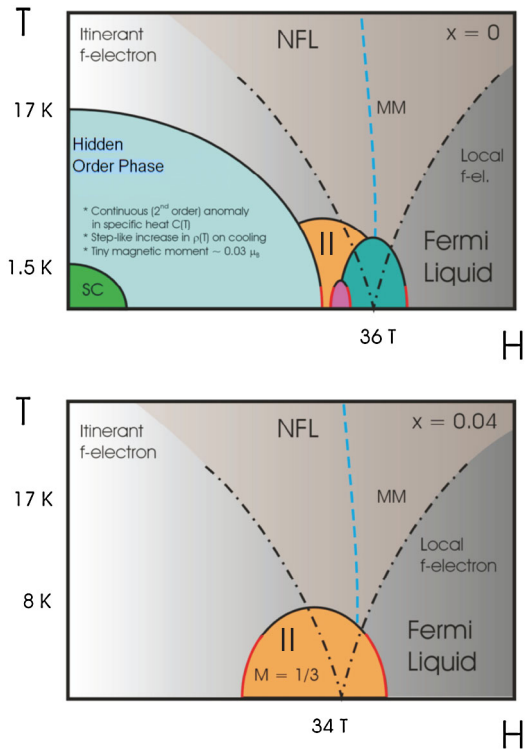

FIG. 12 (color online). Sketch of the high-magnetic-field T-H phase diagrams for URu_2Si_2 and $U(Ru_{0.96}Rh_{0.04})_2Si_2$. MM indicates the metamagnetic transitions, NFL indicates the non-Fermi-liquid, and phase II is also noted. From Jaime, 2007.

Further experiments to examine this magnetic-field-induced critical point were carried out by K. H. Kim *et al.* (2003) via a comprehensive magnetoresistivity study. By plotting continuous variations of $\rho(H)$ at various temperatures and $\rho(T)$ at various fields, they determined the extremities in $d\rho/dH$ and $d\rho/dT$, and by combining these results with the above findings, constructed a complete T-H phase diagram. Figure 12 exhibits this high-field phase diagram with the details of the five distinct phases, three of which are the newly discovered novel phases.

Recent measurements of quantum oscillations in the resistivity, i.e., the SdH effect, by Jo *et al.* (2007), demonstrated the dramatic reconstruction of the Fermi surface when leaving the HO phase and entering phase II spanning the field region around 35 T. The SdH results suggest an increase in the effective carrier concentration, thereby destabilizing the gapping of the itinerant quasiparticles which leads to the increase in the magnetization. The high-field sweeps were also performed under pressure beginning in the LMAF phase and field driven to novel phase formation. Here the high-field phases determined via the resistivity show qualitatively the same number and T-H shapes as the ambient-pressure phases. This means that pressurizing the material from HO to LMAF does not alter the resulting high-field phase formations, again indicating the similar FSs in HO and LMAF. The high-field Fermi-surface reconstruction was further indicated from a combination of resistivity, Hall, and Nernst effect measurements (Levallois *et al.*, 2009).

The effect of Rh doping allows us to simplify the high-field phase diagram. It has been known since the early work of Amitsuka *et al.* (1988) that small amounts of Rh substituted for Ru create puddles of LMAF and suppress the HO via a combination of stress at the larger Rh sites and the addition of an extra 4d electron. Above 4% Rh substitution on the Ru site both HO and LMAF phases are removed, and there is only a heavy-Fermi-liquid (HFL) ground state in low fields, i.e., no ordered phase of any kind. A large magnetic field has been applied to study its effect on the HFL. Kim *et al.* (2004) carried out a systematic study of Rh substitution in $U(Ru_{1-x}Rh_x)_2Si_2$ in fields up to 45 T. The five complicated phases were reduced at $x = 0.04$ to a single field-induced phase: The surviving symmetric domelike shape of phase II spans the field 26 to 37 T with a maximum peak temperature of 9 K. By extrapolation of the HFL behavior of the resistivity and magnetization data from outside the dome to inside, a single point is reached at 0 K and 34 T, again suggesting a field-induced quantum critical point that is suppressed by the formation of a field-induced novel phase. Further analysis of the 4% Rh-doped samples, $U(Ru_{0.96}Rh_{0.04})_2Si_2$, was carried out by Silhanek *et al.* (2005, 2006) using specific-heat and magnetocaloric measurements. Here the high-field novel phase II was mapped out and comparisons drawn with the valency transition in $(Yb_{1-x}Y_x)InCu_4$ and the metamagnetic transformation in $CeRu_2Si_2$. Figure 12 also compares the H-T phase diagram for $U(Ru_{0.96}Rh_{0.04})_2Si_2$ with that of undoped URu_2Si_2. Recently a theoretical description of the

suppression of HO by Rh impurities was presented by Pezzoli *et al.* (2011). They studied the local competition of HO Ψ with LMAF m, where disorder is the driving force of the two competing effects. Accordingly, the phase diagram as a function of x-Rh is obtained and compared with the local LMAF "patch" model derived from ^{29}Si NMR (Baek *et al.*, 2010).

Another way of slowly quenching the HO with doping is to substituted Re for Ru. A recent study (Butch and Maple, 2009) found that $\approx 15\%$ Re substitution leads to a ferromagnetic phase beginning at a putative quantum phase transition. This work suggests the possible formation of a ferromagnetic quantum critical point.

The final aspect of doping the pure URu_2Si_2 compound is to reduce the U concentration to the dilute limit, i.e., $R_{1-x}U_xRu_2Si_2$, where R = Th, La; Y and x is a few percent U. Such investigations were pioneered by Amitsuka and Sakakibara (1994) and spanned a decade of experimentation (Yokoyama *et al.*, 2002). Important questions are posed here. Can dilute U in a nonmagnetic matrix support a single-impurity Kondo effect or even a multichannel Kondo behavior (Cox, 1987)? Are the $5f$ electrons of the single U ion localized and magnetic with a Kondo effect or itinerant, dissolved into the conduction density of states at E_F? As is well known in Kondo physics it would seem that this depends on the particular matrix, Th, La, or V (Marumoto, Takeuchi, and Miyako, 1996). The conclusion after many measurements was ambiguous, however neither of the above two possibilities, conventional or multichannel Kondo effect, was clearly established. Recently this topic has gained renewed interest from both the theoretical and experimental sectors (Toth *et al.*, 2010).

VII. PRESENT STATE OF HO

Particularly strong interest persists today in solving the HO enigma. At present experiment has turned toward repeating some of the previous (20 year old) measurements using the latest advances in experimental methods and crystal growth as, for example, with the aforementioned INS (Bourdarot *et al.*, 2010). Here we consider first the recent progress made in optical conductivity and quantum oscillations. Further experimentation has taken advantage of techniques developed for and effectively utilized in the high-temperature superconductors, viz., scanning tunneling microscopy and spectroscopy (STM and STS), and ARPES which we discuss below. A surge in new theories dedicated to the HO is simultaneously taking place; their current status is surveyed below.

Renewed optical conductivity experiments are currently under way on the new generation of URu_2Si_2 crystals (Levallois *et al.*, 2010; Lobo, Homes, and Lejay, 2010). The goal here is to perform systematic spectroscopy measurements on oriented samples down to lower frequencies and temperatures. Such experiments probed the gradual formation of the hybridization gap which was found to start above 40 K in the KL (HFL) phase, reaching a dip width of ≈ 15 meV as the temperature is reduced toward T_o. Anisotropic reduction of the conductivity was also detected between the a and c axes due to hybridization (Levallois *et al.*, 2010)). Hence, a reconstruction of the electronic structure at 30 K above T_o is

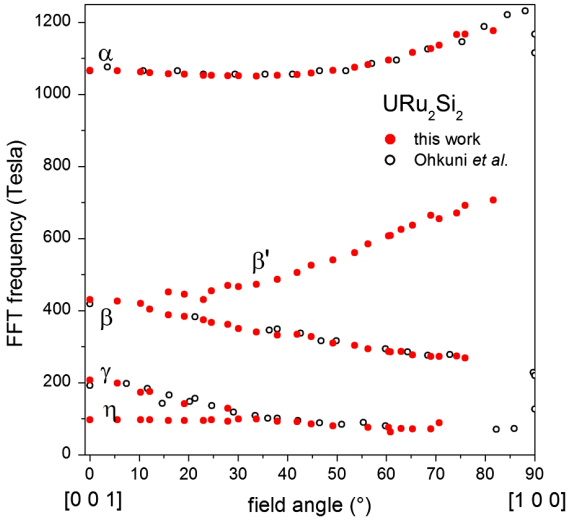

FIG. 13 (color online). Angular dependence of extremal quantum oscillation frequencies in URu_2Si_2, comparing the de Haas–van Alphen data of Ohkuni *et al.* (1999) and the Shubnikov–de Haas data of Hassinger *et al.* (2010) ("this work"). A previously unseen splitting of the β branch was observed, as well as an η orbit that almost coincides with the previously detected γ orbit. Note that the large extremal orbit ε was not detected (cf. Fig. 14). FFT: fast Fourier transform. From Hassinger *et al.*, 2010.

suggested. The opening of the HO gap (expected to be $\approx$ 5 meV or 40^{-1} cm) below T_o has still not been fully determined. Although clearly indicated by Lobo, Homes, and Lejay (2010), in accordance with older measurements (Bonn, Garrett, and Timusk, 1988; Thieme *et al.*, 1995; Degiorgi *et al.*, 1997), it had only recently been observed down to 5 K and 1.2 meV (10 cm^{-1}) in reflectivity (van der Marel, 2011). Further experiments are now in progress to systematically study the optical conductivity below the HO transition.

A new series of Shubnikov–de Haas experiments has just been completed on high-quality single crystals of URu_2Si_2 under pressure (Hassinger *et al.*, 2010) and in high magnetic fields (Altarawneh *et al.*, 2011). The fresh angle-dependent data of Hassinger *et al.* (2010), shown in Fig. 13, reveal two earlier undetected FS branches in the HO phase which has increased the observed enhanced mass to over 50% of that derived from the specific heat. In combination with recent SdH measurements (Shishido *et al.*, 2009), also on a high-purity single crystal, where another new, heavy branch was discovered, we now believe the FS to be definitely established. By increasing the pressure the LMAF was reached and the quantum oscillations were measured and compared to those in the HO state. There was little change in the FS between these two phases. This is unexpected, as the HO and LMAF phases are considered to be separated by a first-order phase transition (Motoyama, Nishioka, and Sato, 2003). The new SdH result supports the conjecture that the lattice doubling and modified Brillouin zone of the LMAF are already present in the HO state. Hence, the suggestion arises that the HO transition breaks bct translational symmetry. There exists agreement of the various angular-dependent FS branches of Hassinger *et al.* (2010) and those predicted from DFT calculations (Oppeneer *et al.*, 2010); the computed FS

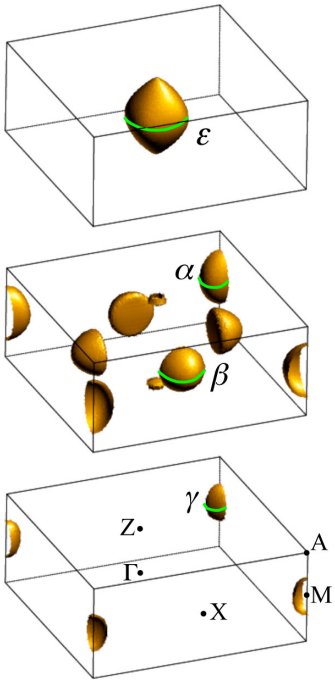

FIG. 14 (color online). Computed Fermi-surface sheets of URu_2Si_2 in the LMAF phase. The extremal Fermi-surface orbits for field along the $z = c^\star$ axis are indicated by lines, and the branches are labeled by greek letters. Not visible is the small Γ-centered ellipsoid (η in Fig. 13) that is inside the large Γ-centered surface in the top panel. High-symmetry points are indicated in the bottom panel. From Elgazzar *et al.*, 2009.

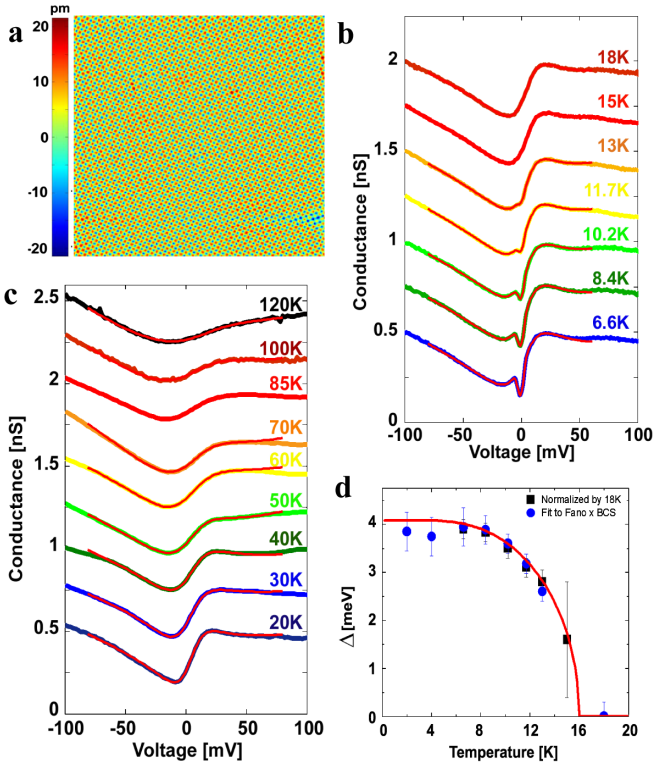

FIG. 15 (color online). STM and STS spectra of URu_2Si_2. (a) Topological image of the measured U-terminated surface (20×20 nm^2). (b) Differential conductance spectrum dI/dV vs V, spanning the HO up to T_o. Note the HO gap appearance within the Fano spectrum. (c) Conductance data from 120 to 20 K illustrating the evolution of the Fano resonance. (d) Measured temperature dependence of the HO gap Δ. The gap displays an asymmetric BCS-like temperature dependence. Adapted from Aynajian *et al.*, 2010.

sheets are shown in Fig. 14 and discussed further below. Thus, we know now the all-important FS of HO URu_2Si_2 and, at least partially, the translational symmetry breaking that occurs.

The recent high-field SdH investigation of Altarawneh *et al.* (2011) found a sequence of four Fermi-surface changes when the field was swept to 40 T. The field-induced modifications of the SdH oscillations were interpreted as a pocket-by-pocket magnetic polarization of the Fermi surface with increasing field, until the HO is destroyed at ∼35 T. In addition, rotating field measurements were employed to determine the effective g factor. Consistent with earlier dHvA experiments (Ohkuni *et al.*, 1999) a highly angle-dependent g factor was obtained, emphasizing the strong Ising-like anisotropy present in URu_2Si_2. The first explanation of the single-ion Ising feature was in terms of the anisotropic Kondo model (Goremychkin *et al.*, 2002). Alternatively, in an itinerant approach it originates from the strong spin-orbit coupling of U which is particularly effective for hybridized states in the presence of a reduced lattice symmetry. This interesting Ising property has not yet received the attention it deserves.

STM and STS have finally succeeded in detecting the atomically resolved properties of the heavy-fermion material URu_2Si_2. Two groups at Cornell (Schmidt *et al.*, 2010) and Princeton (Aynajian *et al.*, 2010), have mastered the art of cold cleaving the compound *in situ* in cryogenic vacuum, thereby obtaining clean, flat surfaces of many tens of nanometers in size for topology and spectroscopy. The issue of surface termination remains unresolved, with Schmidt *et al.* (2010) suggesting a Si top layer. In contrast, based upon many cleaves with different surface reconstructions and their interface steps, Aynajian *et al.* (2010) determined a U surface termination. Once the surface topology was established, the spectroscopy could be performed with atomic resolution to detect locally modulated structures. Figure 15 shows both the topology and the spectroscopy of the atomically resolved U surface termination. Surprisingly, as the temperature was lowered into the Kondo-liquid regime, $T < 100$ K, a Fano line shape developed in the differential conductance dI/dV, Fig. 15(c). Previously this asymmetric line shape had been associated with a single-impurity Kondo resonance due to the two interfering tunneling paths: one through the itinerant electrons, and the other through the Kondo resonance, now the U $5f$ electrons. The width of the Fano spectrum, which varies as a function of temperature, gives an estimate of the Kondo temperature, here ≈ 120 K. The appearance of a Fano line shape in URu_2Si_2 has stimulated a mixture of theoretical descriptions (Haule and Kotliar, 2009; Maltseva, Dzero, and Coleman, 2009; Yang, 2009; Figgins and Morr, 2010; Wölfle, Dubi, and Balatsky, 2010; Dubi and Balatsky, 2011; Yuan, Figgins, and Morr, 2011). As the temperature is further lowered, $T < 17$ K, into the HO state, a clear dip emerges within the Fano structure, i.e., the HO gap Δ_{HO} of ≈ 5 meV appears (Aynajian *et al.*, 2010; Schmidt *et al.*, 2010). Note

the evolution of the Fano resonance below 100 K and the sharp-in-temperature appearance of the HO gap within the Fano spectrum; see Fig. 15(b). $\Delta_{HO}(V, T)$ is asymmetric with respect to the Fermi energy and, most importantly, its temperature dependence mimics a BCS mean-field gap opening. At the lowest temperatures, $T < 4$ K [see Fig. 15(b)], additional structure or modes appear within the HO gap, presenting a new demand for the theory [cf. Dubi and Balatsky (2011)]. By taking advantage of the atomic resolution the spatial modulations in the conductivity can be studied. Both the Fano spectrum and the HO gap are strongest between the U surface atoms. Thus it seems that the main tunneling processes or largest tunneling density of states are into hybridized electronic states that exist in between the U sites, i.e., involving nonlocalized or itinerant $5f$ electrons.

By placing Th impurities on the U surface, Schmidt *et al.* (2010) were able to image quasiparticle interference patterns. When Fourier transformed, the bias voltage versus the **k**-space structure showed the splitting of a light band into two heavy bands as the temperature falls below T_o. Once again the splitting is of the order of 5 meV at $\mathbf{Q} = 0.3a^\star$, consistent with the ensemble of other measurements.

The surge of efforts in the ARPES field is truly remarkable: eight international groups are presently involved in such challenging measurements on URu_2Si_2. Although ARPES is a most successful tool for studying high-temperature superconductors, it has been only moderately effective for strongly correlated electron systems because of their 3D Brillouin zones, their hostile cleaving and surface properties, and the need for very low temperatures, ultrahigh vacuum, and extreme meV resolution. Yet early on two ARPES investigations (Denlinger *et al.*, 2000, 2001; Ito *et al.*, 1999) in the Kondo-liquid (paramagnetic) phase attempted to compare the energy bands mapped from ARPES spectra with those of the band-structure calculations then available (Yamagami, 1998). Here the comparisons were of little use without a direct determination of or correspondence to the U $5f$ bands near and crossing the FS.

A recent ARPES study by Santander-Syro *et al.* (2009) using He-lamp energies (≈ 21 eV) and a high-resolution analyzer has detected and tracked a narrow band of heavy quasiparticles that shifts from above to below the Fermi level as the temperature is reduced through the HO transition. Above E_F the narrow band appears incoherent, yet once below the Fermi level the band sharpens and disperses as a heavy-electron band that seems to be hybridized with a light-hole band at specific **k** values corresponding to the FS of this conduction-electron band. The measured behavior is interpreted as representing a new type of Fermi-surface instability associated with the reconstruction of portions of the FS involving heavy quasiparticles. This work suggests that KL coherence develops at the HO transition and thus not at the coherence temperature $T^\star \approx 70$ K. The specific data treatment applied might, however, play a role here. Hence, this pioneering experiment has given rise to an array of critical questions concerning the data collection method and analysis. Nonetheless, Santander-Syro *et al.* (2009) demonstrated the effectiveness of ARPES in studying the HO transition in URu_2Si_2 and their work has led to the present wave of additional ARPES experiments.

Recently, Yoshida *et al.* (2010) performed laser ARPES using a 6 eV laser source on URu_2Si_2 and $U(Ru_{1-x}Rh_x)_2Si_2$, with $x = 0.03$. The 3% Rh substitution is sufficient to eliminate the HO. This ARPES study, which is mostly sensitive to the d bands, reveals that a narrow, yet dispersive, band suddenly *appears* below E_F when the temperature is lowered to below T_o, a feature that is absent in the Rh-substituted sample. The sudden appearance of this band provides evidence for a doubling of the unit cell along the c axis in the HO, an observation that agrees with that deduced from the latest SdH measurements (Hassinger *et al.*, 2010).

ARPES in the soft-x-ray range was also recently reported (Kawasaki *et al.*, 2011a, 2011b). In this energy range photoemission probes the bulk electronic structure, whereas it is particularly surface sensitive at He I and He II energies. Variation of the photon energy reveals $5f$-related energy bands dispersing in an energy window from -0.6 eV to E_F, which are in good agreement with band-structure calculations assuming itinerant $5f$ electrons. Moreover, these bulk sensitive ARPES measurements do not detect a narrow heavy band in the vicinity of E_F, in contrast to the He I study of Santander-Syro *et al.* (2009). This narrow heavy band is consequently attributed to a surface contribution.

A new technique, time- and angular-resolved photoemission spectroscopy (tr-ARPES), was recently applied to study the dynamics of the HO quasiparticles on the femtosecond time scale (Dakovski *et al.*, 2011). Within reciprocal space the probed position is first tuned to one of the Fermi-surface hot spots (see below), and subsequently the femtosecond time-resolved quasiparticle dynamics at this location is probed after stimulation with a pump laser. Measurements performed below and above T_o reveal that the quasiparticle lifetime dramatically rises by 1 order of magnitude upon entering the HO. The formation of long-lived quasiparticles at the hot spots is identified as the principal mediator of the HO phase. Although the study proved the existence of driving quasiparticles, their precise nature could not yet be disclosed.

Contemporary theory has reconsidered the early band-structure calculations (Norman, Oguchi, and Freeman, 1988; Rozing, Mijnarends, and Koelling, 1991) with the use of state-of-the-art electronic structure methods. Elgazzar *et al.* (2009) performed such calculations on URu_2Si_2 within the framework of DFT within the local density approximation (LDA). While such an approach may be suspect for a strongly correlated electron system, it represents the basic starting point for more sophisticated methods. The calculation was applied to the paramagnetic (or Kondo-liquid) phase and the LMAF phase, in which there is a reasonable magnetic moment ($\sim 0.4\mu_B$) and a conventional antiferromagnetic transition. Here the computed band structure and FS obtained from the energy dispersions showed critical regions or "hot spots" in **k** space where degenerate band crossings at E_F ("Dirac points") induce FS instabilities. These accidental band degeneracies in the normal state, shown in Fig. 16, cause FS gapping when symmetry breaking through antiferromagnetic ordering takes place. Thus, we have the LMAF phase transition. An increase in the exchange interaction leads to a larger magnetic moment and a greater FS gap.

Applying various computational methods to treat the f electron correlations, viz. DFT-LDA, LDA with added strong

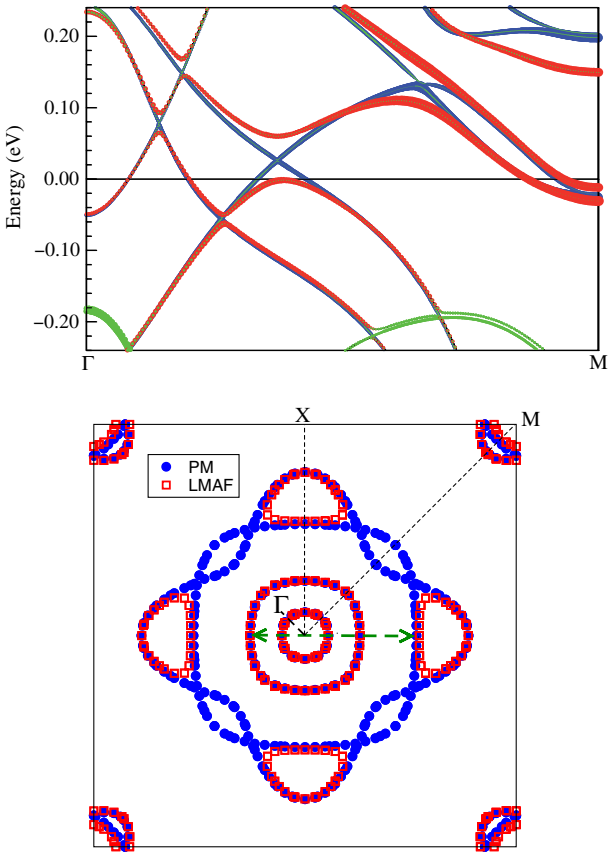

FIG. 16 (color online). Top: Computed energy dispersions of URu_2Si_2 along the Γ-M high-symmetry direction in the simple tetragonal Brillouin zone. The character of the states responsible for the bands is shown through the colors, where the U 5f character in the paramagnetic (PM) normal state, and the U 5f character in the LMAF phase are shown as well as the Ru 4d character. The amount of the Ru d or U f character is provided through the thickness of the bands. Note that energy dispersions for the PM normal state and LMAF phases are almost on top of each other, but a conspicuous lifting of a band degeneracy and a concomitant opening of a gap occurs between Γ and M. Bottom: Cross sections of the PM (circles) and the LMAF (squares) phases in the $k_z = 0$ plane, showing the removal of FS portions in the LMAF phase. The FS sections between the rounded half spheres become completely gapped. Other FS are parts are not affected; the LMAF and PM FS cross sections are almost identical. The dashed arrow indicates the nesting vector $0.4a^\star$ [i.e., $(1 \pm 0.4, 0, 0)$ in the bct structure]. Adapted from Oppeneer *et al.*, 2010.

Coulomb interaction (LDA + U), and dynamical mean-field theory (DMFT), an in-depth comparison of calculated and known experimental properties of the PM and LMAF phases was performed by Oppeneer *et al.* (2010). Good agreement is found throughout when the 5f electrons are treated as itinerant, especially regarding the ordered U moment which is composed of opposite spin and orbital components in accord with the net measured neutron moment of $0.4\mu_B$ (Bourdarot *et al.*, 2003b; Amitsuka *et al.*, 2007; Butch *et al.*, 2010). Hence, the LMAF phase and its FS gapping is understood. Now there remains the difficulty with the HO phase since this phase is not long-range magnetically ordered, i.e., there is no intrinsic HO magnetic moment. Yet we know from experiment that the HO and LMAF phases have quite similar properties, for example, the transport energy gap (Jeffries *et al.*, 2007) and the FS (Nakashima *et al.*, 2003; Hassinger *et al.*, 2010). Therefore, the band-structure calculations should also apply to the HO state, provided appropriate assumptions are made for the origin of the HO. In this phase there are the long-lived, longitudinal, dynamical spin fluctuations observed in the INS resonance. Based upon this commensurate $\mathbf{Q}_0$ spin resonance, Elgazzar *et al.* (2009) proposed a novel dynamical symmetry-breaking model. They argued that the antiferromagnetic spin mode causes the FS gapping and thus drives the HO transition. Here unit-cell doubling along the c axis and time-reversal-symmetry breaking due to a dynamic mode were proposed for the HO in the electronic structure calculations of Elgazzar *et al.* (2009), leading to the FS topology shown in Fig. 14. Detailed DFT calculations of quantum oscillations have recently been performed (Oppeneer *et al.*, 2010). The calculated extremal FS cross sections of the theoretical FS of Fig. 14 are in good agreement with recent experimental data. There are five branches; four of these correspond to the branches detected by Hassinger *et al.* (2010), including the splitting of the β branch. Theory also predicts a larger ε branch (1.35 kT) that was detected by Shishido *et al.* (2009), but not by Hassinger *et al.* (2010). The commensurate spin mode drives the FS gapping and leads to the average gap magnitude as the order parameter and the integrated intensity of the resonance (dynamical susceptibility) as a secondary order parameter. Both order parameters exhibit a BCS-like temperature dependence. A new aspect now enters the theory, namely, the time scale of the spin resonance (Oppeneer *et al.*, 2010). However, the central question persists: Can a dynamical mode create a phase transition?

Balatsky *et al.* (2009) proposed that the incommensurate spin mode at $\mathbf{Q}_1$ would be essential to the HO instead of the antiferromagnetic mode at $\mathbf{Q}_0$. Assuming a coupling between FS sheets connected by the nesting vector $\mathbf{Q}_1$, giving rise to a FS gap in the HO, they derived a form of the dynamic spin susceptibility $\chi(\mathbf{Q}_1, \omega)$ in accordance with INS measurements. Also, Balatsky *et al.* (2009) calculated the temperature-dependent specific heat related to the assumed FS gapping and obtained good agreement with experiment. INS studies of the commensurate spin resonance were reported recently (Bourdarot *et al.*, 2010); similar studies at the incommensurate mode are now required to unveil their distinct contribution and relative importance.

Haule and Kotliar (2009) presented a new theoretical approach to calculate the correlated electronic structure of URu_2Si_2 and related it to the known experimental facts. Using a combination of DFT and temperature-dependent DMFT applied to a U^{4+} $5f^2$ localized configuration, they deduce a CEF scheme consisting of the $\Gamma_1^{(1)}$ and Γ_2 singlets, with a CEF splitting of ≈ 35 K. This level scheme supports a complex order parameter, consisting of a dipolar order J_z and simultaneously a hexadecapolar order, $(J_xJ_y + J_yJ_x) \times (J_x^2 - J_y^2)$. The two-singlets scheme and possible multipoles are those that were considered earlier by Nieuwenhuys (1987) and Santini and Amoretti (1994), except for the reversed order of the ground and first excited states. As the temperature is lowered, the system evolves from this local $5f^2$ configuration into a multichannel Kondo state which at

temperatures lower than 35 K becomes "arrested" by the CEF splitting. The two phases, HO and LMAF, are treated as real and imaginary, respectively, parts of the same OP, and arise from collective CEF excitations to the excited state. Accordingly, the HO phase transition is the formation of the real part of the nonmagnetic hexadecapole OP that breaks rotational symmetry but preserves time-reversal symmetry. Upon tuning, e.g., pressure, the imaginary part of the OP dominates and corresponds to the LMAF phase with its time-reversal-symmetry breaking. Thus this complex OP treats both phases with their different symmetry-breaking properties. Haule and Kotliar (2009) also calculated the one-electron spectral function which they correlate with the recent STM and STS experiments (Aynajian *et al.*, 2010; Schmidt *et al.*, 2010), and their results give the observed Fano resonances. The microscopic DMFT calculations furthermore determine the FS and DOS. These quantities are, however, disparate from those obtained in another recent DMFT calculation that started from a nearly itinerant $5f$ configuration plus a modest Coulomb interaction U (Oppeneer *et al.*, 2010). The FS predicted for a $5f^2$ hexadecapolar state also does not seem to be in correspondence with the recent SdH results (Hassinger *et al.*, 2010).

In order to draw further experimental comparisons, Haule and Kotliar (2010) used the above framework to develop a Landau-Ginzburg theory of the HO in URu_2Si_2. Here they consider phase modifications due to strain, pressure, and magnetic field as has been studied experimentally via uniaxial stress (Yokoyama *et al.*, 2005), thermal expansion (Motoyama *et al.*, 2008), and neutron scattering (Aoki *et al.*, 2009). The theory also associates the INS $\mathbf{Q}_0$ resonance with a pseudo-Goldstone mode which carries a fluctuating magnetic moment in the HO phase as seen in the neutron scattering. The impact of the Haule and Kotliar theory necessitates the experimental search for some evidence of the CEF levels and their splitting, which up until now has not been found. In addition, with newly available x-ray techniques, e.g., x-ray Bragg diffraction (Lovesey *et al.*, 2005) or nonresonance inelastic x-ray scattering, the observation of high-order multipolar transitions might be a future possibility (Gupta *et al.*, 2010).

A different approach by Harima, Miyake, and Flouquet (2010) was to present a space group analysis of the URu_2Si_2 crystal structure and thereby approach the HO transition as a change of crystal symmetry. Based upon group theoretical tabulations, they found that a second-order structural transition occurs from the "mother" space group $I4/mmm$ to $P4_2/mnm$ which does not require a lattice distortion and would keep the NQR frequency at the Ru site unchanged (Saitoh *et al.*, 2005). The analysis is performed within a localized, quadrupolar framework, adopting the Γ_5 doublet to form antiferromagnetic J_xJ_y quadrupoles. In order to detect the proposed charge distribution of quadrupole pairs, greatly improved resonant x-ray sensitivities are needed, since until now there is no firm experimental evidence for quadrupolar formation or its antiferromagnetic long-range order (Amitsuka *et al.*, 2010; Walker *et al.*, 2011).

Along similar lines Su *et al.* (2011) returned to predict a CDW model using the theoretical results of the hybridization wave calculation (Dubi and Balatsky, 2011). Here the primary OP is caused by an incommensurate hybridization between light- and heavy-fermion bands near the Fermi level at $\mathbf{Q} = \pm 0.3a^\star$. The resulting scattering between f electrons and d holes at $\pm\mathbf{Q}$ generates an instability forming a hybridization wave in momentum space. Experimental comparisons are drawn with the Fano resonance and HO gapping from STM and STS (Aynajian *et al.*, 2010; Schmidt *et al.*, 2010). The CDW is in this scenario induced as a secondary order parameter by the primary HO OP. We note that for many years a vast experimental scrutiny to detect a CDW has failed. As a result at the present moment with many innovative efforts the search continues for the solution of the unsolved case of HO in URu_2Si_2.

Recently, Okazaki *et al.* (2011) performed magnetic torque measurements on URu_2Si_2 to determine the magnetic susceptibility in the tetragonal basal plane. They observed a rotational symmetry reduction, from fourfold in the paramagnetic phase to twofold for temperatures below T_o. They interpret this as evidence of a nonzero off-diagonal magnetic susceptibility χ_{xy} in the HO. The torque effect can be found only in one or two tiny single crystals of URu_2Si_2. Okazaki *et al.* (2011) propose that domain formation prevents the detection for larger crystals. Accordingly, this breaking of fourfold rotation symmetry in a tetragonal crystal is suggested to be related to an electronic nematic phase, i.e., a directional electronic state in a heavy-fermion metal [see, e.g., Podolsky and Demler (2005) for a discussion of spin nematic phases]. The possibility of a reduction from tetragonal symmetry was earlier investigated by in-plane oriented thermal expansion measurements, but these could not detect any notable effect, $\Delta L/L < 10^{-7}$ (Kuwahara *et al.*, 1997).

Thalmeier and Takimoto (2011) developed a Landau free energy functional to describe the possible variety of multipolar order parameters that could be compatible with the torque measurement. Their conclusion is that an E-type, (antiferromagnetic) two-component (O_{yz}, O_{zx}) quadrupole can best fit the twofold torque oscillations as the HO symmetry. In addition, based upon the torque results (Okazaki *et al.*, 2011), Pépin *et al.* (2011) proposed spatially modulated spin-liquid order in the basal plane as the HO. Such order is created by a Kondo breakdown critical point. Fujimoto (2011) examined scenarios for a spin nematic state in an effective two-band model with nesting properties of the two bands as given by first-principles calculations. The spin nematic phase is proposed to be a spin-triplet electron-hole pairing state, with electron and hole particles, respectively, located in either one of the two nested bands. This leads to a d-type pairing OP that does not break time-reversal symmetry but has broken fourfold symmetry in the basal plane. Oppeneer *et al.* (2011) proposed that the nonzero off-diagonal susceptibility is caused by dynamical spin-orbital currents circulating around U atoms in the tetragonal planes.

These new results emphasize the question of which symmetry is spontaneously broken in the HO. The recent laser ARPES experiments (Yoshida *et al.*, 2010) suggested doubling of the unit cell along the c axis, in agreement with SdH data which trace a similar FS in both the HO and LMAF (Hassinger *et al.*, 2010). The latest torque measurements suggest a symmetry reduction in the tetragonal plane

(Okazaki *et al.*, 2011). A major question that persists is whether time-reversal symmetry is broken in the HO. Experiments have not been able to conclusively answer this question. Early on, the spurious SMAF phase obscured its clarification, and even current experiments have not provided the final answer. μSR experiments performed in the HO and LMAF phases (Amato *et al.*, 2004) unveiled a peculiar difference: a strongly anisotropic dipolar field along the c axis in the LMAF phase, corresponding to Ising-like order, but a very weak, *isotropic* local field in the HO. This field is not related to a spurious SMAF phase or an inhomogeneous mixing of an LMAF component, as the local field is smaller than that of $0.03\mu_B$ ordered moments, which in addition would be Ising anisotropic. The presence of the internal field could point to a time-odd phase, which is, however, apparently distinct from the long-range dipolar-ordered LMAF phase. A bothersome question is the origin of such a field. Could fluctuations of multipole states or averaging due to a spin fluctuation mode account for this?

What have we now learned about URu_2Si_2 and its HO phase? After a quarter century of investigations seeking to uncover the HO, the identity of this mysterious phase remains unresolved. Yet our understanding of this intriguing heavy-fermion material and the HO has markedly increased. Finally, in 2010, two quantities, the FS gap and the dynamical spin susceptibility, were proven to display mean-field-like OP behavior (Aynajian *et al.*, 2010; Bourdarot *et al.*, 2010). These findings should thus provide a hint as to where to search for the OP. Quantum oscillation measurements established a seemingly complete picture of the FS in the HO (Shishido *et al.*, 2009; Hassinger *et al.*, 2010; Altarawneh *et al.*, 2011). The surprisingly large entropy release at the HO transition could be attributed to a gapping of intensive long-lived spin excitations (Wiebe *et al.*, 2007) which appear to play a critical role (Oppeneer *et al.*, 2010). Here there clearly emerges the dominance of nonlocal, itinerant $5f$ electrons. In addition, at least part of the spontaneous symmetry breaking in the HO has been discovered, as there are now clear indications for unit-cell doubling along the c axis (Yoshida *et al.*, 2010) and a first observation of fourfold rotational symmetry breaking in the basal plane (Okazaki *et al.*, 2011). The high-field and doping behaviors illustrate the fragility of the HO and its uniqueness among heavy-fermion materials. Some of these new observations do call for further investigation and independent confirmation, and, moreover, the interconnections of the various features of the HO need to be clarified. We anticipate that the HO problem will continue to raise questions and challenge our understanding of the spontaneous emergence of new ordered phases of matter.

ACKNOWLEDGMENTS

We gratefully acknowledge discussions with J. W. Allen, H. Amitsuka, P. Aynajian A. V. Balatsky, N. Bernhoeft, M. Biasini, F. Bourdarot, W. J. L. Buyers, R. Caciuffo, P. Chandra, P. Coleman, N. J. Curro, J. D. Denlinger, A. de Visser, T. Durakiewicz, S. Elgazzar, J. Flouquet, M. Graf, H. Harima, N. Harrison, E. Hassinger, K. Haule, M. Jaime, V. Janis, J. R. Jeffries, G. Knebel, G. Kotliar, G. H. Lander, N. Magnani, M. B. Maple, D. van der Marel, Y. Matsuda, K. McEwen, Y. Ōnuki, R. Osborn, C. Pépin, C. Pfleiderer, J. Rusz, A. Santander-Syro, J. Schoenes, M.-T. Suzuki, P. Thalmeier, C. M. Varma, and A. Yazdani. This work has been supported through the Swedish Research Council (VR).

Note added in proof.—After submission of this article several works on URu_2Si_2 appeared. Malone *et al.* (2011) measured its thermoelectric coefficients in a high magnetic field and suggested that changes of the Fermi surface topology occur deep in the HO phase at high fields. Liu *et al.* (2011) employed ultrafast pump-probe optical spectroscopy to monitor the response to a fs-laser pulse. The decay of the optical pumped state suggests the opening of a pseudogap below 25 K. Theoretical support for this idea was provided by Haraldsen *et al.* (2011) who deduced the presence of a pseudogap state from PCS measurements. Toth and Kotliar (2011) proposed a localized hexadecapolar Kondo effect in diluted URu_2Si_2. Further, the most recent experimental studies on URu_2Si_2 are by Niklowitz *et al.* (2011), who performed quasielastic scattering from the $\mathbf{Q}_0$ and $\mathbf{Q}_1$ resonances, Bourdarot *et al.* (2011), who performed neutron scattering under uniaxial stress, and Nagel *et al.* (2011), who made a Fermi liquid analysis of the optical conductivity.

REFERENCES

Altarawneh, M. M., N. Harrison, S. E. Sebatian, L. Balicas, P. H. Tobash, J. D. Thompson, F. Ronning, and E. D. Bauer, 2011, Phys. Rev. Lett. **106**, 146403.

Amato, A., M. J. Graf, A. de Visser, H. Amitsuka, D. Andreica, and A. Schenck, 2004, J. Phys. Condens. Matter **16**, S4403.

Amitsuka, H., K. Hyomi, T. Nishioka, Y. Miyako, and T. Suzuki, 1988, J. Magn. Magn. Mater. **76–77**, 168.

Amitsuka, H., T. Inami, M. Yokoyama, S. Takayama, Y. Ikeda, I. Kawasaki, Y. Homma, H. Hidaka, and T. Yanagisawa, 2010, J. Phys. Conf. Ser. **200**, 012007.

Amitsuka, H., K. Matsuda, I. Kawasaki, K. Tenya, M. Yokoyama, C. Sekine, N. Tateiwa, T. C. Kobayashi, S. Kawarazaki, and H. Yoshizawa, 2007, J. Magn. Magn. Mater. **310**, 214.

Amitsuka, H., and T. Sakakibara, 1994, J. Phys. Soc. Jpn. **63**, 736.

Amitsuka, H., M. Sato, N. Metoki, M. Yokoyama, K. Kuwahara, T. Sakakibara, H. Morimoto, S. Kawarazaki, Y. Miyako, and J. A. Mydosh, 1999, Phys. Rev. Lett. **83**, 5114.

Aoki, D., F. Bourdarot, E. Hassinger, G. Knebel, A. Miyake, S. Raymond, V. Taufour, and J. Flouquet, 2009, J. Phys. Soc. Jpn. **78**, 053701.

Aynajian, P., E. H. da Silva Neto, C. V. Parker, Y.-K. Huang, A. Pasupathy, J. A. Mydosh, and A. Yazdani, 2010, Proc. Natl. Acad. Sci. U.S.A. **107**, 10 383.

Baek, S.-H, M. J. Graf, A. V. Balatsky, E. D. Bauer, J. C. Cooley, J. L. Smith, and N. J. Curro, 2010, Phys. Rev. B **81**, 132404.

Balatsky, A. V., A. Chantis, H. P. Dahal, D. Parker, and J. X. Zhu, 2009, Phys. Rev. B **79**, 214413.

Barzykin, V., and L. P. Gor'kov, 1993, Phys. Rev. Lett. **70**, 2479.

Barzykin, V., and L. P. Gor'kov, 1995, Phys. Rev. Lett. **74**, 4301.

Behnia, K., *et al.*, 2005, Phys. Rev. Lett. **94**, 156405.

Bel, R., H. Jin, K. Behnia, J. Flouquet, and P. Lejay, 2004, Phys. Rev. B **70**, 220501(R).

Bernal, O. O., M. E. Moroz, K. Ishida, H. Murakawa, A. P. Reyes, P. L. Kuhns, D. E. MacLaughlin, J. A. Mydosh, and T. J. Gortenmulder, 2006, Physica B (Amsterdam) **378–380**, 574.

Bernal, O. O., C. Rodrigues, A. Martinez, H. G. Lukefahr, D. E. MacLaughlin, A. A. Menovsky, and J. A. Mydosh, 2001, Phys. Rev. Lett. **87**, 196402.
Biasini, M., J. Rusz, and A. P. Mills, 2009, Phys. Rev. B **79**, 085115.
Bonn, D. A., J. D. Garrett, and T. Timusk, 1988, Phys. Rev. Lett. **61**, 1305.
Bourdarot, F., *et al.*, 2005, Physica B (Amsterdam) **359–361**, 986.
Bourdarot, F., B. Fåk, K. Habicht, and K. Prokes, 2003a, Phys. Rev. Lett. **90**, 067203.
Bourdarot, F., B. Fåk, V. P. Minnev, M. E. Zhitomirsky, N. Kernavanois, S. Raymond, P. Burlet, F. Lapierre, P. Lejay, and J. Flouquet, 2003b, arXiv:cond-mat/0312206v1.
Bourdarot, F., E. Hassinger, S. Raymond, D. Aoki, V. Taufour, L.-P. Regnault, and J. Flouquet, 2010, J. Phys. Soc. Jpn. **79**, 064719.
Bourdarot, F., *et al.*, 2011, arXiv:1110.5157.
Broholm C., J. K. Kjems, W. J. L. Buyers, P. Matthews, T. T. M. Palstra, A. A. Menovsky, and J. A. Mydosh, 1987, Phys. Rev. Lett. **58**, 1467.
Broholm C., H. Lin, P. T. Matthews, T. E. Mason, W. J. L. Buyers, M. F. Collins, A. A. Menovsky, J. A. Mydosh, and J. K. Kjems, 1991, Phys. Rev. B **43**, 12 809.
Butch, N. P., J. R. Jeffries, S. Chi, J. Batista Leão, J. W. Lynn, and M. B. Maple, 2010, Phys. Rev. B **82**, 060408(R).
Butch, N. P., and M. B. Maple, 2009, Phys. Rev. Lett. **103**, 076404.
Buyers, W. J. L., 1996, Physica B (Amsterdam) **223–224**, 9.
Chandra, P., P. Coleman, J. A. Mydosh, and V. Tripathi, 2002, Nature (London) **417**, 831.
Coleman, P., and A. J. Schofield, 2005, Nature (London) **433**, 226.
Cox, D. L., 1987, Phys. Rev. Lett. **59**, 1240.
Cricchio, F., F. Bultmark, O. Grånäs, and L. Nordström, 2009, Phys. Rev. Lett. **103**, 107202.
Dakovski, G. L., *et al.*, 2011, Phys. Rev. B **84**, 161103(R).
Dalla Torre, E. G., E. Berg, and E. Altman, 2006, Phys. Rev. Lett. **97**, 260401.
de Boer, F. R., J. J. M. Franse, E. Louis, A. A. Menovsky, J. A. Mydosh, T. T. M. Palstra, U. Rauchschwalbe, W. Schlabitz, F. Steglich, and A. de Visser, 1986, Physica B (Amsterdam) **138**, 1.
Degiorgi, L., St. Thieme, H. R. Ott, M. Dressel, G. Grüner, Y. Dalichaouch, M. B. Maple, Z. Fisk, C. Geibel, and F. Steglich, 1997, Z. Phys. B **102**, 367.
Denlinger, J. D., G.-H. Geweon, J. W. Allen, C. G. Olson, M. B. Maple, J. L. Sarrao, P. E. Armstrong, Z. Fisk, and H. Yamagami, 2001, J. Electron Spectrosc. Relat. Phenom. **117–118**, 347.
Denlinger, J. D., G.-H. Gweon, J. W. Allen, C. G. Olson, Y. Dalichaouch, B.-W. Lee, M. B. Maple, Z. Fisk, P. C. Canfield, and P. E. Armstrong, 2000, Physica B (Amsterdam) **281–282**, 716.
de Visser, A., F. E. Kayzel, A. A. Menovsky, J. J. M. Franse, J. van den Berg, and G. J. Nieuwenhuys, 1986, Phys. Rev. B **34**, 8168.
Dubi, Y., and A. V. Balatsky, 2011, Phys. Rev. Lett. **106**, 086401.
Elgazzar, S., J. Rusz, M. Amft, P. M. Oppeneer, and J. A. Mydosh, 2009, Nature Mater. **8**, 337.
Escudero, R, F. Morales, and P. Lejay, 1994, Phys. Rev. B **49**, 15 271.
Fazekas, P., A. Kiss, and K. Radnóczi, 2005, Prog. Theor. Phys. Suppl. **160**, 114.
Figgins, J., and D. Morr, 2010, Phys. Rev. Lett. **104**, 187202.
Fisher, R. A., S. Kim, Y. Wu, N. E. Phillips, M. W. McElfresh, M. S. Torikachvili, and M. B. Maple, 1990, Physica B (Amsterdam) **163**, 419.
Fujimoto, S., 2011, Phys. Rev. Lett. **106**, 196407.
Goremychkin, E. A., R. Osborn, B. D. Rainford, T. A. Costi, A. P. Murani, C. A. Scott, and P. J. C. King, 2002, Phys. Rev. Lett. **89**, 147201.
Gor'kov, L. P., 1991, Europhys. Lett. **16**, 301.
Gor'kov, L. P., and A. Sokol, 1992, Phys. Rev. Lett. **69**, 2586.
Gupta, S. S., J. A. Bradely, M. W. Haverkort, G. T. Seidler, A. Tanaka, and G. A. Sawatzky, 2010, arXiv:cond-mat/1001.5293v1.
Hanzawa, K., 2007, J. Phys. Condens. Matter **19**, 072202.
Hanzawa, K., and N. Watanabe, 2005, J. Phys. Condens. Matter **17**, L419.
Haraldsen, J. T., Y. Dubi, N. J. Curro, and A. V. Balatsky, 2011, arXiv:1104.2931.
Harima, H., K. Miyake, and J. Flouquet, 2010, J. Phys. Soc. Jpn. **79**, 033705.
Harrison, N., M. Jaime, and J. A. Mydosh, 2003, Phys. Rev. Lett. **90**, 096402.
Hasan, M. Z., and C. L. Kane, 2010, Rev. Mod. Phys. **82**, 3045.
Hasselbach, K., J. R. Kirtley, and P. Lejay, 1992, Phys. Rev. B **46**, 5826.
Hassinger, E., J. Derr, J. Levallois, D. Aoki, K. Behnia, F. Bourdarot, G. Knebel, C. Proust, and J. Flouquet, 2008, J. Phys. Soc. Jpn. **77**, Suppl. A, 172.
Hassinger, E., G. Knebel, K. Izawa, P. Lejay, B. Salce, and J. Flouquet, 2008, Phys. Rev. B **77**, 115117.
Hassinger, E., G. Knebel, T. D. Matsuda, D. Aoki, V. Taufour, and J. Flouquet, 2010, Phys. Rev. Lett. **105**, 216409.
Haule, K., and G. Kotliar, 2009, Nature Phys. **5**, 796.
Haule, K., and G. Kotliar, 2010, Europhys. Lett. **89**, 57006.
He, R.-H., *et al.*, 2011, Science **331**, 1579.
Hill, J. A., 1970, in *Plutonium and Other Actinides*, edited by N. W. Miner (The Metallurgical Society of the AIME, New York).
Ikeda, H., and Y. Ohashi, 1998, Phys. Rev. Lett. **81**, 3723.
Isaacs, E. D., D. B. McWhan, R. N. Kleiman, D. J. Bishop, G. E. Ice, P. Zschack, B. D. Gaulin, T. E. Mason, J. D. Garrett, and W. J. L. Buyers, 1990, Phys. Rev. Lett. **65**, 3185.
Ito, T., H. Kumigashira, T. Takahashi, Y. Haga, E. Yamamoto, T. Honma, H. Ohkuni, and Y. Ōnuki, 1999, Phys. Rev. B **60**, 13 390.
Jaime, M., 2007 (unpublished).
Jaime, M., K. H. Kim, G. Jorge, S. McCall, and J. A. Mydosh, 2002, Phys. Rev. Lett. **89**, 287201.
Janik, J. A., 2008, Ph.D. thesis, Florida State University (unpublished).
Janik, J. A., *et al.*, 2009, J. Phys. Condens. Matter **21**, 192202.
Jeffries, J. R., N. P. Butch, B. T. Yukich, and M. B. Maple, 2007, Phys. Rev. Lett. **99**, 217207.
Jeffries, J. R., N. P. Butch, B. T. Yukich, and M. B. Maple, 2008, J. Phys. Condens. Matter **20**, 095225.
Jeffries, J. R., K. T. Moore, N. P. Butch, and M. B. Maple, 2010, Phys. Rev. B **82**, 033103.
Jo, Y. J., L. Balicias, C. Capan, K. Behnia, P. Lejay, J. Flouquet, J. A. Mydosh, and P. Schlottmann, 2007, Phys. Rev. Lett. **98**, 166404.
Kasahara, Y., T. Iwasawa, H. Shishido, T. Shibauchi, K. Behnia, Y. Haga, T. D. Matsuda, Y. Ōnuki, M. Sigrist, and Y. Matsuda, 2007, Phys. Rev. Lett. **99**, 116402.
Kasahara, Y., H. Shishido, T. Shibauchi, Y. Haga, T. D. Matsuda, Y. Ōnuki, and Y. Matsuda, 2009, New J. Phys. **11**, 055061.
Kasuya, T., 1997, J. Phys. Soc. Jpn. **66**, 3348.
Kawasaki, I., S.-i. Fujimori, Y. Takeda, T. Okane, A. Yasui, Y. Saitoh, H. Yamagami, Y. Haga, E. Yamamoto, and Y. Onuki, 2011a, J. Phys. Conf. Ser. **273**, 012039.
Kawasaki, I., S.-i. Fujimori, Y. Takeda, T. Okane, A. Yasui, Y. Saitoh, H. Yamagami, Y. Haga, E. Yamamoto, and Y. Onuki, 2011b, Phys. Rev. B **83**, 235121.
Kim, J. S., D. Hall, P. Kumar, and G. R. Stewart, 2003, Phys. Rev. B **67**, 014404.

Kim, K. H., N. Harrison, H. Amitsuka, G. A. Jorge, M. Jaime, and J. A. Mydosh, 2004, Phys. Rev. Lett. **93**, 206402.
Kim, K. H., N. Harrison, M. Jaime, G. S. Boebinger, and J. A. Mydosh, 2003, Phys. Rev. Lett. **91**, 256401.
Kiss, A., and P. Fazekas, 2005, Phys. Rev. B **71**, 054415.
Kohori, Y., K. Matsuda, and T. Kohara, 1996, J. Phys. Soc. Jpn. **65**, 1083.
Kotetes, P., A. Aperis, and G. Varelogiannis, 2010, arXiv:cond-mat/1002.2719.
Kotetes, P., and G. Varelogiannis, 2010, Phys. Rev. Lett. **104**, 106404.
Kuramoto, Y., H. Kusunose, and A. Kiss, 2009, J. Phys. Soc. Jpn. **78**, 072001.
Kusunose, H., and H. Harima, 2011, J. Phys. Soc. Jpn. **80**, 084702.
Kuwahara, K., H. Amitsuka, T. Sakakibara, O. Suzuki, S. Nakamura, T. Goto, M. Mihalik, A. A. Menovsky, A. de Visser, and J. J. M. Franse, 1997, J. Phys. Soc. Jpn. **66**, 3251.
Kuwahara, K., M. Koghi, K. Iwasa, M. Nishi, K. Nakajima, M. Yokoyama, and H. Amitsuka, 2006, Physica B (Amsterdam) **378–380**, 581.
Levallois, J., K. Behnia, J. Flouquet, P. Lejay, and C. Proust, 2009, Europhys. Lett. **85**, 27 003.
Levallois, J., F. Lévy-Bertrand, M. K. Tran, J. A. Mydosh, Y.-K. Huang, and D. van der Marel, 2010, arXiv:cond-mat/1007.538.
Liu, M. K. , *et al.*, 2011, Phys. Rev. B **84**, 161101(R).
Lobo, R., C. C. Homes, and P. Lejay, 2010 (private communication).
Lovesey, S. W., E. Balcar, K. S. Knight, and J. Fernández Rodríguez, 2005, Phys. Rep. **411**, 233.
Luke, G. M., A. Keren, L. P. Le, Y. J. Uemura, W. D. Wu, D. Bonn, L. Taillefer, J. D. Garrett, and Y. Onuki, 1994, Hyperfine Interact. **85**, 397.
MacLaughlin, D. E., *et al.*, 1988, Phys. Rev. B **37**, 3153.
Malone, L., *et al.*, 2011, Phys. Rev. B **83**, 245117.
Maltseva, M., M. Dzero, and P. Coleman, 2009, Phys. Rev. Lett. **103**, 206402.
Manna, R. S., M. de Souza, A. Brühl, J. A. Schlueter, and M. Lang, 2010, Phys. Rev. Lett. **104**, 016403.
Maple, M. B., J. W. Chen, Y. Dalichaouch, T. Kohara, C. Rossel, M. S. Torikachvili, M. W. McElfresh, and J. D. Thompson, 1986, Phys. Rev. Lett. **56**, 185.
Marumoto, K., T. Takeuchi, and Y. Miyako, 1996, Phys. Rev. B **54**, 12 194.
Mason, T. E., W. J. L. Buyers, T. Petersen, A. A. Menovsky, and J. D. Garrett, 1995, J. Phys. Condens. Matter **7**, 5089.
Mason, T. E., B. D. Gaulin, J. D. Garrett, Z. Tun, W. J. L. Buyers, and E. D. Isaacs, 1990, Phys. Rev. Lett. **65**, 3189.
Matsuda, K., Y. Kohori, and T. Kohara, 1996, J. Phys. Soc. Jpn. **65**, 679.
Matsuda, K., Y. Kohori, T. Kohara, H. Amitsuka, K. Kuwahara, and T. Matsumoto, 2003, J. Phys. Condens. Matter **15**, 2363.
Matsuda, K., Y. Kohori, T. Kohara, E. K. Kuwahara, and H. Amitsuka, 2001, Phys. Rev. Lett. **87**, 087203.
Matsuda, T. D., D. Aoki, S. Ikeda, E. Yamamoto, Y. Haga, H. Ohkuni, R. Settai, and Y. Ōnuki, 2008, J. Phys. Soc. Jpn. **77**, Suppl. A, 362.
Matsuda, T. D., *et al.*, 2011, J. Phys. Soc. Jpn. **80**, 114710.
McElfresh, M. W., J. D. Thompson, J. O. Willis, M. B. Maple, T. Kohara, and M. S. Torikachvili, 1987, Phys. Rev. B **35**, 43.
Mihalik, M., A. Kolomiets, J.-C. Griveau, A. V. Andreev, and V. Sechovský, 2006, High Press. Res. **26**, 479.
Mineev, V. P., and M. E. Zhitomirsky, 2005, Phys. Rev. B **72**, 014432.
Moore, K. T., and G. van der Laan, 2009, Rev. Mod. Phys. **81**, 235.
Morales, F., and R. Escudero, 2009, J. Low Temp. Phys. **154**, 68.
Motoyama, G., T. Nishioka, and N. K. Sato, 2003, Phys. Rev. Lett. **90**, 166402.
Motoyama, G., N. Yokoyama, A. Sumiyama, and Y. Oda, 2008, J. Phys. Soc. Jpn. **77**, 123710.
Nagel, U., *et al.*, 2011, arXiv:1107.5574.
Nakashima, M., H. Ohkuni, Y. Inada, R. Setti, Y. Haga, E. Yamamoto, and Y. Ōnuki, 2003, J. Phys. Condens. Matter **15**, S2011.
Nieuwenhuys, G. J., 1987, Phys. Rev. B **35**, 5260.
Niklowitz, P. G., C. Peiderer, T. Keller, M. Vojta, Y.-K. Huang, and J. A. Mydosh, 2010, Phys. Rev. Lett. **104**, 106406.
Niklowitz, P. G., *et al.*, 2011, arXiv:1110.5599.
Norman, M. R., T. Oguchi, and A. J. Freeman, 1988, Phys. Rev. B **38**, 11 193.
Oh, Y. S., K.-H. Kim, P. A. Sharma, N. Harrison, H. Amitsuka, and J. A. Mydosh, 2007, Phys. Rev. Lett. **98**, 016401.
Ohkawa, F., and H. Shimizu, 1999, J. Phys. Condens. Matter **11**, L519.
Ohkuni, H., Y. Tokiwa, K. Sakurai, R. Settai, T. Haga, E. Yamamoto, Y. Ōnuki, H. Yamagami, S. Takahashi, and T. Yanagisawa, 1999, Philos. Mag. B **79**, 1045.
Okazaki, R., Y. Kasahara, H. Shishido, M. Konczykowski, K. Behnia, Y. Haga, T. D. Matsuda, Y. Onuki, T. Shibauchi, and Y. Matsuda, 2008, Phys. Rev. Lett. **100**, 037004.
Okazaki, R., T. Shibauchi, H. J. Shi, Y. Haga, T. D. Matsuda, E. Yamamoto, Y. Onuki, H. Ikeda, and Y. Matsuda, 2011, Science **331**, 439.
Okuno, Y., and K. Miyake, 1998, J. Phys. Soc. Jpn. **67**, 2469.
Oppeneer, P. M., J. Rusz, S. Elgazzar, M.-T. Suzuki, T. Durakiewicz, and J. A. Mydosh, 2010, Phys. Rev. B **82**, 205103.
Oppeneer, P. M., S. Elgazzar, J. Rusz, Q. Feng, T. Durakiewicz, and J. A. Mydosh, 2011, arXiv:1110.0981.
Ott, H. R., H. Rudigier, Z. Fisk, and J. L. Smith, 1983, Phys. Rev. Lett. **50**, 1595.
Paixão, J. A., C. Detlefs, M. J. Longfield, R. Caciuffo, P. Santini, N. Bernhoeft, J. Rebizant, and G. H. Lander, 2002, Phys. Rev. Lett. **89**, 187202.
Palstra, T. T. M., A. A. Menovsky, and J. A. Mydosh, 1986, Phys. Rev. B **33**, 6527(R).
Palstra, T. T. M., A. A. Menovsky, J. van den Berg, A. J. Dirkmaat, P. H. Kes, G. J. Nieuwenhuys, and J. A. Mydosh, 1985, Phys. Rev. Lett. **55**, 2727.
Pépin, C., M. R. Norman, S. Burdin, and A. Ferraz, 2011, Phys. Rev. Lett. **106**, 106601.
Pezzoli, M. E., M. J. Graf, K. Haule, G. Kotliar, and A. V. Balatsky, 2011, Phys. Rev. B **83**, 235106.
Pfleiderer, C., 2009, Rev. Mod. Phys. **81**, 1551.
Pfleiderer, C., J. A. Mydosh, and M. Vojta, 2006, Phys. Rev. B **74**, 104412.
Podolsky, D., and E. Demler, 2005, New J. Phys. **7**, 59.
Ramirez, A. P., P. Coleman, P. Chandra, E. Brück, A. A. Menovsky, Z. Fisk, and E. Bucher, 1992, Phys. Rev. Lett. **68**, 2680.
Rodrigo, J. G., F. Guinea, S. Vierira, and F. G. Aliev, 1997, Phys. Rev. B **55**, 14 318.
Rozing, G. J., P. E. Mijnarends, and D. D. Koelling, 1991, Phys. Rev. B **43**, 9515.
Saitoh, S., S. Takagi, M. Yokoyama, and H. Amitsuka, 2005, J. Phys. Soc. Jpn. **74**, 2209.
Santander-Syro, A. F., M. Klein, F. L. Boariu, A. Nuber, P. Lejay, and F. Reinert, 2009, Nature Phys. **5**, 637.
Santini, P., 1998, Phys. Rev. B **57**, 5191.
Santini, P., and G. Amoretti, 1994, Phys. Rev. Lett. **73**, 1027.
Santini, P., and G. Amoretti, 1995, Phys. Rev. Lett. **74**, 4098.

Santini, P., S. Carretta, G. Amoretti, R. Caciuffo, N. Magnani, and G. H. Lander, 2009, Rev. Mod. Phys. **81**, 807.
Santini, P., S. Carretta, N. Magnani, G. Amoretti, and R. Caciuffo, 2006, Phys. Rev. Lett. **97**, 207203.
Santini, P., R. Lémanski, and P. Erdös, 1999, Adv. Phys. **48**, 537.
Sato, H., 2008, J. Phys. Soc. Jpn. **77**, Suppl. A, 1.
Schlabitz, W., J. Baumann, R. Pollit, U. Rauchschwalbe, H. M. Mayer, U. Ahlheim, and C. D. Bredl, 1986, Z. Phys. B **62**, 171.
Schmidt, A. R., M. H. Hamidian, P. Wahl, F. Meier, A. V. Balatsky, J. D. Garrett, T. J. Williams, G. M. Luke, and J. C. Davis, 2010, Nature (London) **465**, 570.
Schoenes, J., C. Schönenberger, J. J. M. Franse, and A. A. Menovsky, 1987, Phys. Rev. B **35**, 5375.
Sechovský, V., and L. Havela, 1998, in *Handbook of Magnetic Materials*, edited by K. H. J. Buschow (Elsevier Science, Amsterdam, The Netherlands), Vol. 11, p. 1.
Shah, N., P. Chandra, P. Coleman, and J. A. Mydosh, 2000, Phys. Rev. B **61**, 564.
Sharma, P. A., N. Harrison, M. Jaime, Y. S. Oh, K. H. Kim, C. D. Batista, H. Amitsuka, and J. A. Mydosh, 2006, Phys. Rev. Lett. **97**, 156401.
Shishido, H., *et al.*, 2009, Phys. Rev. Lett. **102**, 156403.
Sikkema, A. E., W. J. L. Buyers, I. Affleck, and J. Gan, 1996, Phys. Rev. B **54**, 9322.
Silhanek, A. V., N. Harrison, C. D. Batista, M. Jaime, A. Lacerda, H. Amitsuka, and J. A. Mydosh, 2005, Phys. Rev. Lett. **95**, 026403.
Silhanek, A. V., N. Harrison, C. D. Batista, M. Jaime, A. Lacerda, H. Amitsuka, and J. A. Mydosh, 2006, Physica B (Amsterdam) **378–380**, 373.
Silhanek, A. V., *et al.*, 2006, Phys. Rev. Lett. **96**, 136403.
Smith, J. L., and E. A. Kmetko, 1983, J. Less-Common Met. **90**, 83.
Stewart, G. R., 2001, Rev. Mod. Phys. **73**, 797.
Stewart, G. R., 2006, Rev. Mod. Phys. **78**, 743.
Stewart, G. R., Z. Fisk, J. O. Willis, and J. L. Smith, 1984, Phys. Rev. Lett. **52**, 679.
Su, J.-J., Y. Dubi, P. Wölfe, and A. V. Balatsky, 2011, J. Phys. Condens. Matter **23**, 094214.
Sugiyama, K., H. Fuke, K. Kindo, K. Shimohata, A. A. Menovsky, J. A. Mydosh, and M. Date, 1990, J. Phys. Soc. Jpn. **59**, 3331.
Suzuki, M.-T., N. Magnani, and P. M. Oppeneer, 2010, Phys. Rev. B **82**, 241103(R).
Takagi, S., S. Ishihara, S. Saitoh, H.-I. Sasaki, H. Tanida, M. Yokoyama, and H. Amitsuka, 2007, J. Phys. Soc. Jpn. **76**, 033708.
Thalmeier, P., and T. Takimoto, 2011, Phys. Rev. B **83**, 165110.
Thieme, St., P. Steiner, L. Degiorgi, P. Wachter, Y. Dalichaouch, and M. B. Maple, 1995, Europhys. Lett. **32**, 367.
Tokunaga, Y., Y. Homma, S. Kambe, D. Aoki, H. Sakai, E. Yamamoto, A. Nakamura, Y. Shiokawa, R. E. Walstedt, and H. Yasuoka, 2005, Phys. Rev. Lett. **94**, 137209.
Toth, A., P. Chandra, P. Coleman, G. Kotliar, and H. Amitsuka, 2010, Phys. Rev. B **82**, 23516.
Toth, A. P., and G. Kotliar, 2011, arXiv:1106.5768.
Tripathi, V., P. Chandra, and P. Coleman, 2005, J. Phys. Condens. Matter **17**, 5285.
Valla, T., A. V. Fedorov, J. Lee, J. C. Davis, and G. D. Gu, 2006, Science **314**, 1914.
van der Marel, D., 2011 (private communication).
Varma, C. M., and L. Zhu, 2006, Phys. Rev. Lett. **96**, 036405.
Villaume, A., F. Bourdarot, E. Hassinger, S. Raymond, V. Taufour, D. Aoki, and J. Flouquet, 2008, Phys. Rev. B **78**, 012504.
Walker, H. C., R. Caciuffo, D. Aoki, F. Bourdarot, G. H. Lander, and J. Flouquet, 2011, Phys. Rev. B **83**, 193102.
Walker, H. C., K. A. McEwen, D. F. McMorrow, S. B. Wilkins, F. Wastin, E. Colineau, and D. Fort, 2006, Phys. Rev. Lett. **97**, 137203.
Walker, M. B., and W. J. L. Buyers, 1995, Phys. Rev. Lett. **74**, 4097.
Walker, M. B., W. J. L. Buyers, Z. Tun, W. Que, A. A. Menovsky, and J. D. Garrett, 1993, Phys. Rev. Lett. **71**, 2630.
Walter, U., C.-K. Loong, M. Loewenhaupt, and W. Schlabitz, 1986, Phys. Rev. B **33**, 7875(R).
Wiebe, C. R., *et al.*, 2007, Nature Phys. **3**, 96.
Wiebe, C. R., G. M. Luke, Z. Yamani, A. A. Menovsky, and W. J. L. Buyers, 2004, Phys. Rev. B **69**, 132418.
Wolf, B., W. Sixl, R. Graf, D. Finsterbusch, G. Bruls, B. Lüthi, E. A. Knetsch, A. A. Menovsky, and J. A. Mydosh, 1994, J. Low Temp. Phys. **94**, 307.
Wölfle, P., Y. Dubi, and A. V. Balatsky, 2010, Phys. Rev. Lett. **105**, 246401.
Xu, G., *et al.*, 2007, Science **317**, 1049.
Yamagami, H., 1998, J. Phys. Soc. Jpn. **67**, 3176.
Yamagami, H., and N. Hamada, 2000, Physica B (Amsterdam) **284–288**, 1295.
Yang, Y.-F., 2009, Phys. Rev. B **79**, 241107.
Yang, Y.-F., Z. Fisk, H.-O. Lee, J. D. Thompson, and D. Pines, 2008, Nature (London) **454**, 611.
Yano, K., T. Sakakibara, T. Tayama, M. Yokoyama, H. Amitsuka, Y. Homma, P. Miranović, M. Ichioka, Y. Tsutsumi, and K. Machida, 2008, Phys. Rev. Lett. **100**, 017004.
Yokoyama, M., H. Amitsuka, K. Kenya, K. Watanabe, S. Kawarazaki, H. Yoshizawa, and J. A. Mydosh, 2005, Phys. Rev. B **72**, 214419.
Yokoyama, M., H. Amitsuka, K. Kuwahara, K. Tenya, and T. Sakakibara, 2002, J. Phys. Soc. Jpn. **71**, 3037.
Yoshida, R., *et al.*, 2010, Phys. Rev. B **82**, 205108.
Yuan, T., J. Figgins, and D. K. Morr, 2011, arXiv:cond-mat/1101.263v1.